Energy Conversion and Management: X 29 (2026) 101504

Contents lists available at ScienceDirect

Energy Conversion and Management: X

journal homepage: www.sciencedirect.com/journal/energy-conversion-and-management-x

Exploring the impact of synergistic oxygen and waste heat utilization from electrolysis in supporting a climate-neutral energy infrastructure in Germany

Luka Bornemann *, Wolfram Tuschewitzki, Martin Kaltschmitt

Institute of Environmental Technology and Energy Economics, Hamburg University of Technology, Eissendorfer Strasse 40, 21073 Hamburg, Germany

ARTICLE INFO

Dataset link: https://doi.org/10.5281/zenodo.17241332, Code and data for paper: Exploring the impact of synergistic oxygen and waste heat utilization from electrolysis in supporting a climate-neutral energy infrastructure in Germany (Original data)

Keywords:
Green hydrogen
Electrolysis
Oxygen
Waste heat
Energy system optimization
Energy system modeling

ABSTRACT

Hydrogen is considered a key energy carrier for comprehensive defossilization of energy systems, yet large-scale deployment of electrolyzer-based production faces significant cost barriers. The utilization of electrolyzer by-products – oxygen and waste heat – offers a promising approach to reduce production costs. This study addresses whether joint oxygen and waste heat utilization generates synergistic economic benefits within a spatially optimized energy infrastructure – a question unaddressed in prior literature that examined these by-products exclusively in isolation – and provides novel insights into how market mechanisms, electrolyzer siting decisions, and conventional supply infrastructure are affected. These effects are assessed in a cost-optimal cross-sectoral German energy system at high spatial resolution. The analysis reveals that joint by-product utilization achieves near-perfect additive cost savings: 1.9% reduction in total annual system costs and 13% reduction in levelized cost of hydrogen, combining waste heat benefits (1.1% system costs, 9.6% hydrogen costs) and oxygen benefits (0.9% system costs, 4.2% hydrogen costs). These reductions are achieved through partial substitution of conventional supply infrastructure, while enabling novel economically viable production processes (e.g., oxy-fuel processes). However, oxygen utilization's substantial system-level benefits do not adequately translate into electrolyzer operator revenues, limiting private investment incentives. By-product utilization fundamentally alters electrolyzer siting through distinct spatial patterns – short-distance redistribution for waste heat and supraregional shifts for oxygen – while creating synergy hotspots where joint utilization enables novel economically viable production sites. The study demonstrates considerable potential of joint by-product utilization for reducing hydrogen production costs, but realizing this potential requires significant changes in energy supply infrastructure and coordinated cross-sectoral planning to align private decision-making with system-optimal outcomes.

1. Introduction

The global transition to climate neutrality requires large-scale deployment of "green" hydrogen [1] produced through water electrolysis powered by renewable energy [2], with projected global hydrogen demand reaching 148 to 660 Mt/a by 2050 [3] to support defossilizing both the future energy supply and fossil-fuel based industrial processes. However, hydrogen-based energy systems exhibit low overall efficiencies which pose a fundamental barrier to large-scale deployment. Water electrolysis requires substantial energy input, while conversion losses throughout the hydrogen production, storage, and utilization chain result in considerable energy dissipation [4]. These inherent inefficiencies translate directly into high operational costs for hydrogen-based energy systems, including elevated hydrogen production costs that currently hinder economic competitiveness [5]. To improve system efficiency and thus reduce operational costs, various strategies are presented in the literature.

One of these strategies involves the utilization of electrolyzer by-products oxygen and waste heat. Water electrolysis inherently generates ca. 8 kg of oxygen per kg of hydrogen, alongside recoverable waste heat equivalent to ca. 15% of electrical energy input [4]. Both by-products can substitute conventional energy and feedstock supply and motivate the implementation of novel processes. For example, oxygen from electrolyzers can replace oxygen from air separation units (ASUs), whose production process is highly energy-intensive [6], in industrial applications (e.g., steel, glass, pulp, medical [7]). In addition, electrolyzer oxygen can facilitate the development of novel pure oxygen applications (e.g., oxy-fuel combustion [8], wastewater treatment [9]). Moreover, waste heat at 60 to 80 °C [4] can supply district heating networks [10], industrial low-temperature processes [11], or medium-temperature applications up to 200 °C when upgraded via heat pumps [12]. Consequently, the utilization of electrolyzer by-

* Corresponding author.
E-mail address: luka.bornemann@tuhh.de (L. Bornemann).

https://doi.org/10.1016/j.ecmx.2025.101504
Received 30 October 2025; Received in revised form 15 December 2025; Accepted 26 December 2025
Available online 5 January 2026

Nomenclature

Sets

$\mathcal{C}$	Set of all components
$\mathcal{E}$	Set of all commodities
$\mathcal{N}$	Set of all nodes
$\mathcal{T}$	Set of all time steps

Latin letters

c	Price [€/kWh]
D	Specific mass demand [t/t_{prod}]
$\dot{E}$	Commodity flow [kW; kg/h]
E	Amount of commodity [kWh; kg]
M	Molar mass [g/mol]
n	Amount of substance [mol]
P	Electricity demand [kWh]
p	Specific electricity demand [kWh/kg]
q	Per capita wastewater production rate [L/(d pers)]

Greek letters

Δ	Difference [–]

Superscripts and subscripts

BM	Biomass
c	Component
CH_4	Methane
D	Demand
d	Daily
e	Commodity
EL	Electrolyzer
el	Electricity
H_2	Hydrogen
n	Node
O_2	Oxygen
oxy	Oxy-fuel combustion
prod	Product
t	Time step
WH	Waste heat
wwt	Wastewater treatment

Abbreviations

ASU	Air separation unit
BOxD	Biochemical oxygen demand
CAPEX	Capital expenditures
CC	Carbon capture
HHV	Higher heating value
HVC	High-value chemicals
LCOH	Levelized costs of hydrogen
LHV	Lower heating value
PV	Photovoltaic
SOTE	Standard oxygen transfer efficiency
TAC	Total annualized system costs
WH	Waste heat
WWT	Wastewater treatment

products provides both system-wide and electrolyzer-specific benefits by reducing cross-sectoral energy consumption [9] and generating additional revenue streams [13], respectively.

Cost-optimal hydrogen production sites typically concentrate in regions with abundant low-cost renewable energy resources and storage capacities, whereas major by-product demand centers cluster in established urban-industrial regions often distant from these renewable energy-rich zones [14]. Germany provides a particularly instructive case study for examining these dynamics. The country's renewable resources and storage capacities concentrate in northern regions with abundant wind power and salt cavern storage availability, while major industrial and urban demand centers cluster in western and southern Germany [15]. This geographical misalignment between production and utilization sites introduces infrastructure trade-offs that may constrain the potential of by-product utilization. Isolated case studies [16–19] focusing on distinct local energy systems and assuming co-location of electrolyzers and by-product consumers cannot adequately capture these trade-offs. Consequently, a comprehensive, spatially resolved approach is required to evaluate the actual economic viability of by-product utilization within a system-optimized energy infrastructure and to derive critical implications for infrastructure planning decisions.

Existing research on electrolyzer by-product utilization has examined oxygen and waste heat independently but with distinct limitations detailed in Table 1. Oxygen utilization studies focus on isolated industrial applications [16,17,20–23] or system-level assessments [24,25] of oxygen alone, demonstrating levelized cost of hydrogen (LCOH) reductions of 0.2 to 0.9 €/kg for standalone applications and system-level cost savings up to 1.3%. Waste heat utilization research remains confined to case studies that assume co-location of electrolyzers with heat consumers [13,18,19,26–29], reporting efficiency improvements up to 12% and LCOH reductions of up to 11%.

While these studies demonstrate the technical feasibility and economic potential of individual by-product utilization, they exhibit two critical limitations. First, most assume co-location of electrolyzers and by-product demand, thus, neglecting the impact of the spatial mismatch of cost-optimal hydrogen production and by-product demands on national infrastructure planning. The spatial mismatch between low-cost renewable electricity availability and by-product demand centers implies that findings based on co-located setups cannot be extrapolated to the national level. In system-level scenarios, multiple site characteristics compete for electrolyzer capacity allocation and infrastructure investment. This neglect may lead to an overestimation of the potential benefits of by-product utilization.

Our previous study [24] examined oxygen utilization within the German energy system at the national scale and demonstrated system-wide cost reductions through redistribution of electrolyzer capacities towards oxygen demand clusters. However, it only considered oxygen in isolation, which leads to the second and most critical limitation: No existing study examines the combined utilization of oxygen and waste heat within a comprehensive, spatially explicit energy system model. This gap leaves fundamental questions unanswered: (1) Do synergistic effects exist when both by-products are valorized simultaneously, or do combined savings fall short of the sum of individual benefits due to misalignment of demand patterns? (2) Do market mechanisms provide sufficient incentives for electrolyzer operators to adopt by-product utilization strategies that are system-optimal but potentially suboptimal from the operator's economic perspective? (3) How do competing demands for electrolyzer capacity allocation affect system-optimal electrolyzer siting? (4) To what extent can the utilization of by-products substitute conventional supply options, and how significantly do demand patterns change as a result?

To address these research questions, this study employs PyPSA-Eur [30], an open-source, high-resolution energy system optimization framework. Building on our previous work [24], PyPSA-Eur is extended to include a detailed representation of waste heat utilization and additional oxygen applications linked to heat supply. The enhanced optimization model is applied to the German energy system under the framework conditions of achieving climate neutrality by 2045. In total, four scenarios are defined to determine the extent

Table 1
Overview of existing literature in the field of electrolyzer by-product utilization.

Study	By-products	Scope	Co-location	Spatial resolution	Case study
Assunção et al. [16]	Oxygen	Local	Yes	Single site	Oxygen liquefaction plant
Maggio et al. [17]	Oxygen	Local	Yes	Single site	Local energy system
Nhuchhen et al. [23]	Oxygen	Local	Yes	Single site	Cement plant
Campbell-Stanway et al. [25]	Oxygen	Local	Yes	–	Electrolyzer & electricity supply
Bornemann et al. [24] (previous work)	Oxygen	National	No	90 nodes	German energy system
Frassl et al. [18]	Waste heat	Local	Yes	Single site	Local energy system
van der Roest et al. [19]	Waste heat	Local	Yes	Single site	Local energy system
Meriläinen et al. [13]	Waste heat	Local	Yes	Single site	Local energy system
Pompodakis et al. [29]	Waste heat	Local	Yes	Single site	Local energy system
Galvan-Cara and Bongartz [26]	Waste heat	Local	Yes	Single site	Local energy system
This study	Oxygen & waste heat	National	No	110 nodes	German energy system

to which electrolyzer by-products can be utilized (i.e., no utilization, isolated utilization, and joint utilization). For each scenario, a co-optimization of system design and operation is performed across five interconnected sectors (i.e., electricity, heating, industry, transport, and biomass). Comparing these scenarios in terms of infrastructure capacities, spatial redistribution patterns, integrated commodity flows, total annual system costs, and the levelized cost of hydrogen allows the study to quantify the benefits and implications of combined electrolyzer waste heat and oxygen utilization. Unlike previous studies, evaluating isolated and joint utilization within a consistent system-wide model enables a precise attribution of infrastructure effects to each by-product and reveals whether system-level benefits translate into operator-level advantages. This integrated, spatially explicit modeling approach yields the following novel contributions compared to previous literature in the field of electrolyzer by-product utilization.

1. **Economic effects and potential synergies of combined by-product utilization.** Using a high-resolution spatial optimization model of the German energy system, the analysis examines whether joint oxygen and waste heat utilization generates additive, superadditive, or subadditive cost savings relative to their isolated utilization pathways. The study identifies the mechanisms driving synergy or interference between by-products and, in contrast to previous isolated assessments (Table 1), provides new insights into competitive versus complementary interactions across economic and infrastructural dimensions.
2. **Divergence between system-level and operator-level economics.** The energy system model encompasses five interconnected sectors. Unlike previous studies, which only considered individual applications, this cross-sector approach allows to identify not only direct substitution effects but also indirect cross-sector changes in the energy infrastructure. Moreover, the model endogenously generates marginal prices for both by-products based on a cost-optimal energy supply infrastructure and operation. This eliminates the need for exogenous price assumptions common in prior studies. Consequently, enabling modeling both system-level (i.e., energy system perspective) total annual cost impacts and operator-level (i.e., electrolyzer operator perspective) LCOH effects, this work aims to reveal whether by-product utilization leads to similar benefits at both system-level and operator-level, and whether indirect (i.e., cross-sectoral) benefits are adequately captured in market prices and electrolyzer operator revenues. This investigation directly informs policy design to which extent targeted interventions (e.g., by-product production subsidies, industrial retrofit incentives, infrastructure coordination mechanisms) are needed to align private decision-making with system-optimal outcomes.
3. **High-resolution spatial analysis of electrolyzer capacity redistribution driven by competing by-product demands.** Most existing studies assume co-location of electrolyzers and by-product consumers and therefore cannot capture how by-product utilization influences electrolyzer siting. The spatial granularity of this work enables the identification of localized trade-offs between cost-effective hydrogen production and by-product utilization. This includes whether waste heat and oxygen utilization create distinct or overlapping spatial electrolyzer redistribution patterns, and whether synergy hotspots exist where industrial sites with oxygen demand coincide with urban heating loads, enabling economically viable joint utilization that would not be feasible for either by-product alone. This spatial analysis aims to provide infrastructure planners with quantitative guidance on optimal electrolyzer placement strategies.
4. **Impacts on competing commodity supply infrastructure.** The cross-sector approach not only includes competing supply technologies but also allocates constrained resources (e.g., biomass, CO_2 capture) across sectors. This introduces both price and resource competition (e.g., biomass-based heat supply), enabling deeper insights into the structural implications of by-product utilization for conventional supply systems. The analysis quantifies the extent to which by-products substitute conventional infrastructure (e.g., ASUs for oxygen, air-source heat pumps for heating) and how they reshape demand patterns. This reveals infrastructure transition requirements and clarifies whether conventional supply capacities can be retired or must remain as backup, directly informing investment strategies for hydrogen developers and conventional suppliers facing potential market displacement.

By providing this comprehensive assessment, the study aims to offer actionable insights for policymakers, infrastructure planners, and

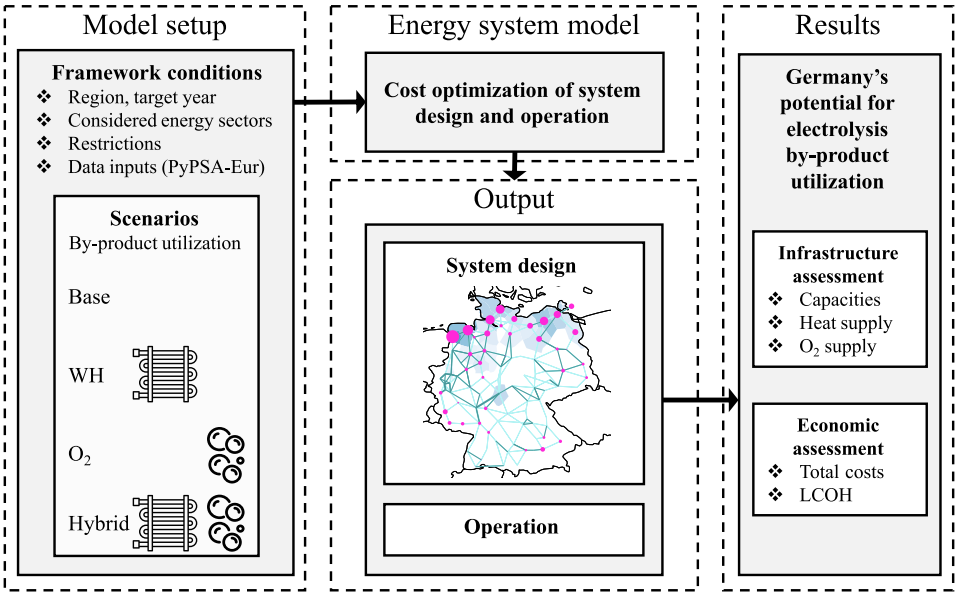

Fig. 1. Methodological approach (adapted from [24], LCOH: levelized cost of hydrogen, WH: waste heat).

electrolyzer operators who face imminent investment decisions. These decisions must be made before infrastructure lock-in effects constrain the potential for economically efficient by-product utilization within Germany's future energy system.

The remainder of this paper is structured as follows. Section 2 outlines the overarching methodological approach, including the energy system model, its extensions, and the applied assessment criteria. Section 3 details the model setup, including the overarching framework conditions and the investigated scenarios. The results and discussion are presented in Section 4, followed by conclusions in Section 5.

2. Methodological approach

This section provides an overview of the methodological approach, including the applied energy system optimization model and the evaluation criteria. Further details on the model setup (e.g., boundary conditions, model assumptions) are presented in Section 3. The methodological framework used to address the research questions is illustrated in Fig. 1. To assess the impacts of electrolyzer by-product utilization, four scenarios are developed that define the extent to which these by-products can be used. Together with overarching framework conditions and system assumptions, these scenarios are implemented within an optimization model of the German energy system. The model co-optimizes system design and operation across all sectors, with the analysis focusing in particular on heat supply, oxygen supply, and hydrogen infrastructure, as well as the resulting total system costs and LCOH.

2.1. Energy system model

This section outlines the fundamental modeling approach and its operational structure. All input parameters referenced in this section are described in detail in Section 3. This work employs PyPSA-Eur [14], an open-source capacity expansion optimization framework for the European energy system. The framework performs simultaneous optimization of investment decisions and operational strategies across the European energy system. Through linear optimization, the model minimizes total annual system costs (TAC), which comprise annualized capital expenditures (CAPEX) and fixed/variable operational expenditures (OPEX) for all modeled components, while satisfying operational constraints (i.e., transmission limitations, energy demands, carbon emission boundaries). The model version (v. 0.11) applied in this work follows a greenfield approach. This implies that, for a given target year and its associated boundary conditions, the optimization determines an entirely new energy system configuration from scratch.

The framework incorporates endogenous commodity demands across multiple sectors (e.g., electricity, transport, heating, industry, agriculture). Based on these demands, it determines the local expansion and operation of generation, storage, conversion, and transmission infrastructure for various commodities (e.g., electricity, heat, biomass, carbon, methane, hydrogen, liquid hydrocarbons) within the European energy system. Its representation accounts for both spatial and temporal characteristics of commodity demand patterns and renewable resource availability throughout Europe. Regional nodes serve as spatial allocation units for commodity demand, renewable potential, and infrastructure parameters, with a temporal resolution down to 1 h. Overall, the framework determines a cost-optimal cross-sectoral European energy system by simultaneously optimizing technology capacities, spatial deployment, and operational strategies under user-defined boundary conditions. The mathematical formulation can be found in Appendix A.1. The boundary conditions, model assumptions, and data sets applied in this work are further outlined in Section 3.

2.1.1. Waste heat framework extensions

The existing waste heat modeling framework in PyPSA-Eur is extended in this study. In its original form, the model only allowed for two options: either dissipating waste heat into the environment as a loss or feeding it into central heating networks. However, waste heat can also be utilized in medium-temperature industrial processes. Therefore, a second utilization pathway is introduced in this work, enabling the use of waste heat for industrial applications by coupling it with a high-temperature heat pump. The extension includes several key modifications to the original modeling framework. First, a dedicated waste heat bus is introduced to enable the flexible allocation of available waste heat across different utilization pathways. Second, a high-temperature heat pump is integrated to facilitate the use of low-temperature waste heat for industrial medium-temperature applications. Third, competing industry heating technologies are added, since medium-temperature industrial heat supply was originally fixed to biomass-based combustion in the standard model. Finally, the medium-temperature industrial heat load is subdivided into two temperature ranges, 100 to 150 °C and 150 to 500 °C (not relevant to waste heat), to allow for a more accurate representation of process-specific temperature requirements.

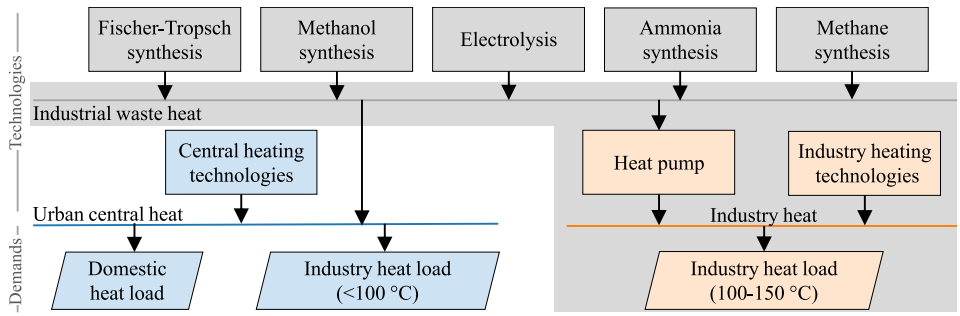

Fig. 2. Waste heat modeling framework, including the modeling extensions highlighted in gray. Block colors indicate different utilization pathways. Gray: waste heat supply technologies; Blue: direct use; Orange: industrial process use.

The extended framework is illustrated in Fig. 2. Industrial processes serving as waste heat sources include electrolysis and the syntheses processes of Fischer–Tropsch, methanol, ammonia, and methane (cf. gray blocks in Fig. 2). The waste heat generated from these processes can be utilized through two distinct pathways.

- The first pathway (cf. blue blocks in Fig. 2) involves direct integration into urban district heating networks, where the waste heat supplies domestic heating loads (i.e., water heating, space heating) and low-temperature industrial process heat below 100 °C (e.g., hot water applications in food processing [11]). Complementary technologies for this application include air-source heat pumps, natural gas boilers and combined heat and power (CHP) units, wood chip CHP systems (all featuring optional carbon capture capabilities), electric resistance heating systems and heat storages.
- The second pathway (cf. orange blocks in Fig. 2) utilizes high-temperature heat pumps to elevate the temperature level of the waste heat, enabling the supply of industrial process heat demands of up to 150 °C (e.g., steam generation for paper, food, and chemical industries [11], cf. Section 3.1 for considered applications). Alternative technologies considered for meeting this demand include electric boilers as well as natural gas and wood chip boilers (incorporating optional carbon capture options).

Further details on the mathematical formulation and the techno-economic parameters of the waste heat framework are provided in Appendix A.2.

2.1.2. Oxygen framework extensions

The oxygen modeling framework builds on the approach introduced in [24]. However, consistent with the extended waste heat framework described in Section 2.1.1, several enhancements are implemented to broaden the scope of oxygen utilization. Specifically, the extensions include the integration of biomass-based oxy-fuel combustion processes for industrial heat supply – where previously only methane-based oxy-fuel combustion was represented – and the incorporation of oxy-fuel combined heat and power (CHP) units within the urban central heating sector. Further, the extensions of the industry heat (cf. Section 2.1.1) also intersect with the oxygen framework. The resulting extended framework is illustrated in Fig. 3.

Oxygen demand is divided into a spatially resolved, exogenous conventional demand and an extended demand resulting endogenously from optimization. The conventional demand (cf. blue block in Fig. 3) reflects current industrial oxygen applications (e.g., steel, glass, healthcare) and represents a fixed, non-flexible baseline that must be fulfilled by the corresponding supply infrastructure. In contrast, the extended demand is modeled as an optional component, allowing the model to decide whether and to what extent new oxygen applications are adopted. This demand includes the retrofit of industrial combustion processes to oxy-fuel combustion (cf. orange and green blocks in Fig. 3),

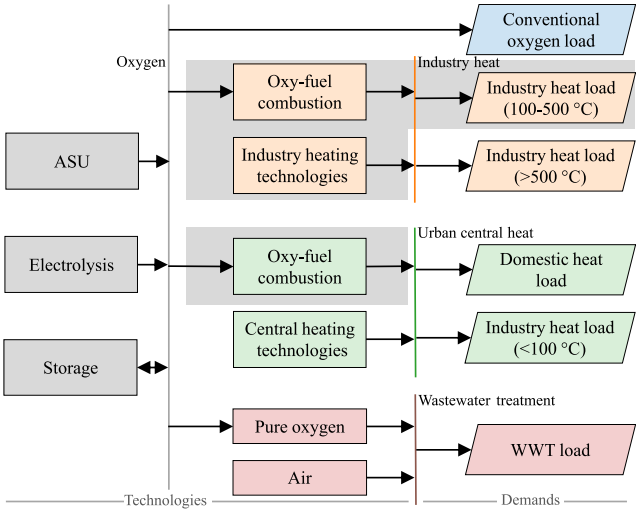

Fig. 3. Oxygen modeling framework, including the modeling extensions highlighted in gray. Block colors indicate different utilization pathways. Gray: oxygen supply technologies; Blue: conventional use; Orange: industrial heat; Green: urban central heat; Violet: wastewater treatment. (ASU: air separation unit, WWT: wastewater treatment).

as well as the use of pure oxygen instead of air in wastewater treatment (cf. violet blocks in Fig. 3). Both process conversions result in reduced energy consumption (i.e., electricity or methane/biomass) and, in the case of oxy-fuel combustion, higher carbon capture rates. Such applications are not yet widely implemented but are technically mature and can be deployed if economically viable. They are therefore represented as potential demand that materializes only when the associated benefits outweigh the costs.

Regarding the achievable improvements through oxy-fuel combustion, a distinction is made between methane-based high-temperature process heat above 500 °C (e.g., steel, cement industries), biomass-based medium-temperature process heat between 100 to 500 °C (e.g., pulp, food industries), and CHP plants for district heating. All oxy-fuel combustion processes include carbon capture capabilities (cf. Section 3.1 for underlying parameters).

The oxygen demand can be covered by oxygen from ASUs and electrolyzers. In addition to oxygen, ASUs also generate other industrial gases as co-products, among which argon is explicitly represented in the modeling framework. Argon is chosen because, given its absolute demand in combination with its relatively low production ratio compared to oxygen, it constitutes the most restrictive co-product with regard to the minimum required ASU capacities [31]. Accordingly, a national, inelastic argon demand is implemented alongside the spatially resolved oxygen demand to capture this restriction, ensuring that ASUs

cannot be fully substituted by electrolyzers. Storage technologies are included for both oxygen and argon to allow temporal balancing between production and demand, while surplus quantities can be vented. Further details on the mathematical formulation and the techno-economic parameters of the oxygen framework are provided in Appendix A.3.

2.2. Evaluation criteria

The assessment of electrolysis by-product utilization potential is performed through infrastructure and economic evaluations.

The infrastructure assessment encompasses the following parameters:

- Total installed capacities of ASUs, electrolyzers and other heat supply technologies, including spatial electrolyzer capacity distributions.
- Total heat provision by electrolyzers and complementary heat supply technologies along with the respective end-use applications.
- Total oxygen generation by ASUs and electrolyzers, the fraction of electrolyzer-produced oxygen that can be incorporated into evolving demand structures, and the associated industrial end-users.

The economic assessment addresses the following parameters:

- Total annual costs (TAC) (i.e., investment and operational expenses) for the national energy system.
- The average national and regional LCOH.

Eq. (1) determines the TAC. The TAC are calculated as the sum of the annualized investment costs $CAPEX_{n,c}$ of all energy system components ($\forall c \in C$; i.e., generation, storage, and transmission) and their operational costs at each node ($\forall n \in \mathcal{N}$). The operational costs comprise the costs of energy conversion for each component and energy carrier ($\forall e \in \mathcal{E}$), where $c_{n,t,e}$ represents the specific conversion costs (e.g., biomass procurement costs) and $\dot{E}^{\mathrm{c}}_{n,t,e}$ denotes the dispatch of the respective component at time step t. The operational costs are calculated for each time step and multiplied by the corresponding time step length Δt_t.

$$TAC = \sum_{n\in\mathcal{N}} \sum_{c\in C} \left(CAPEX_{n,c} + \sum_{t\in\mathcal{T}} \Delta t_t \sum_{e\in\mathcal{E}} c_{n,t,e} \dot{E}^{\mathrm{c}}_{n,t,e} \right) \tag{1}$$

The LCOH are determined using Eq. (2). The calculation incorporates annualized capital expenditures $CAPEX_{n,c}$ for hydrogen-related infrastructure ($\forall c \in C^{\mathrm{H_2}} = \{\text{electrolyzers}\}$), electricity costs for electrolyzer operation, and revenues generated from oxygen and waste heat commercialization. Electricity costs are calculated by multiplying the regional electricity marginal price $c_{n,t,el}$ at each time step ($t \in \mathcal{T}$) by the regional electricity consumption of electrolyzers $\dot{E}^{\mathrm{EL}}_{n,t,el}$. Revenue from oxygen commercialization represents the product of the annual average regional oxygen marginal price $c_{n,\mathrm{O_2}}$ and the regionally integrated electrolysis oxygen $\dot{E}^{\mathrm{EL}}_{n,t,\mathrm{O_2}}$. An analogous calculation applies to waste heat commercialization using the annual average regional waste heat marginal price $c_{n,WH}$ and the regionally integrated electrolysis waste heat $\dot{E}^{\mathrm{EL}}_{n,t,WH}$. These components are aggregated across all time steps, weighted by the time step duration Δt_t, and summed across all nodes ($\forall n \in \mathcal{N}$), then normalized by the total hydrogen demand $E^{\mathrm{D}}_{\mathrm{H_2}}$ to determine the LCOH. The value of oxygen and waste heat (i.e., marginal prices) is determined endogenously via the shadow prices of their respective nodal balance constraints to reflect the systemic benefit. Exogenous price floors or revenue bands are not incorporated.

$$\begin{aligned} LCOH = \frac{1}{E^{\mathrm{D}}_{\mathrm{H_2}}} \sum_{n\in\mathcal{N}} \Bigg(& \sum_{c\in C^{\mathrm{H_2}}} CAPEX_{n,c} \\ & + \sum_{t\in\mathcal{T}} \Delta t_t \left(c_{n,t,el} \dot{E}^{\mathrm{EL}}_{n,t,el} - c_{n,\mathrm{O_2}} \dot{E}^{\mathrm{EL}}_{n,t,\mathrm{O_2}} \right. \\ & \left. - c_{n,WH} \dot{E}^{\mathrm{EL}}_{n,t,WH} \right) \Bigg) \end{aligned} \tag{2}$$

3. Model setup

The following sections outline the system assumptions, boundary conditions, and data sets that form the basis of the energy system model, and introduce the scenarios assessed in this study. All assumptions are applied consistently across all scenarios.

3.1. System assumptions and framework conditions

The following section presents the system assumptions and framework conditions applied in this study, including overarching boundary conditions, technological assumptions, demand structures, as well as spatial and temporal model characteristics.

3.1.1. General boundary conditions

Germany serves as the geographical focus of this work, enabling comprehensive, high-spatial examination of electrolysis by-product utilization while maintaining manageable computational demands. The core framework conditions and system assumptions are adopted from [24]. The model is set for the year 2045, consistent with Germany's target of achieving climate neutrality by that time [32]. As a result, the system-wide CO_2 emissions must be net zero. However, localized CO_2 emissions (e.g., arising from energy conversion or industrial processes) are permitted, provided they are fully compensated through CO_2 removal technologies such as direct air capture and/or point source carbon capture and subsequent storage.

3.1.2. Technology assumptions

For process-related emissions and industrial heat provision, a carbon capture rate of 90% is assumed, while a rate of 95% is applied to heat and electricity generation via CHP [33]. In the case of industrial combustion processes based on methane or biomass, a conversion to oxy-fuel combustion enables an enhanced capture rate of 97% [34], along with efficiency improvements of 15% for methane-based and 10% for biomass-based systems. These improvements reflect both fuel savings due to more efficient combustion and productivity [35] and less energy-intensive carbon capture [36]. For CHPs, only the improved capture rate is considered. Overall, the availability of carbon capture and storage is constrained to a maximum of 100 Mt/a, with associated annual storage costs of 10 €/t [33]. Carbon capture, transport and storage is implemented on a national level and not further spatially resolved. Additional carbon capture and storage limits are evaluated as part of a sensitivity analysis in Appendix B.

Hydrogen supply is restricted to electrolysis. Hydrogen storage is represented by salt cavern facilities, and transmission is modeled via pipeline infrastructure using either repurposed natural gas assets or newly built hydrogen pipelines. The utilization of electrolysis waste heat and oxygen follows the specifications in Sections 2.1.1 and 2.1.2.

Electricity transmission is constrained by linearized DC power flow limits, while hydrogen transport is enabled through an optimizable pipeline network. Heat and oxygen balances are strictly nodal; no inter-nodal transport technologies are modeled for these commodities.

3.1.3. Demands

To reflect realistic hydrogen production and the associated availability of electrolyzer by-products, the analysis encompasses all hydrogen- and by-product-relevant sectors (i.e., electricity, heating, industry, biomass, transport). Hydrogen demand is modeled for both current and emerging applications. This includes its direct use as a feedstock in industrial processes (e.g., steel production, liquid hydrocarbons, synthetic methane, ammonia synthesis). Additionally, prospective future applications are considered, such as the use of hydrogen and its derivatives within the transport sector (i.e., maritime, aviation) and for power generation using fuel cells and gas turbines.

Heat demand is subdivided by region into urban, rural, and industrial-site shares. To analyze electrolysis waste heat utilization in greater detail, the industrial medium-temperature process heat demand (100 to 500 °C) is further split into 100 to 150 °C and 150 to 500 °C bands. Only the 100 to 150 °C band can be supplied by electrolysis waste heat via heat pumps (cf. modeling framework overview in Section 2.1.1). According to current German industrial process heat demand patterns, the temperature range of 100 to 200 °C accounts for roughly 72% of total medium-temperature industrial heat demand [11]. In the absence of a more detailed breakdown, this demand is assumed to be uniformly distributed across the range. This implies that the 100 to 150 °C segment represents ca. 36% of total medium-temperature industrial process heat demand.

The conventional oxygen demand represents current industrial and medical uses (i.e., steel [37,38], pulp [39], basic chemicals [40], other industrial sectors [41], healthcare [42]) and is inelastic. For the extended oxygen demand, process heat provision is assumed retrofittable to oxy-fuel combustion across the steel, high-value chemicals (HVC), cement, alumina, pulp and paper, textiles and leather, food, and wood and wood products industries [24]. The extended oxygen demand is elastic, as it results endogenously from optimization. Further techno-economic parameters related to the extended oxygen applications are presented in Table A.5.

3.1.4. Spatial and temporal resolution

The model represents Germany with 110 nodes, offering a high spatial resolution necessary to adequately capture local heat and oxygen demands and to reflect the spatial proximity of electrolyzer sites to these demands. This resolution provides sufficient detail while maintaining computational tractability. To ensure feasibility on the temporal side, the model aggregates 2045 time-series data (e.g., demand patterns and renewable energy supply) into 3 h intervals, a resolution sufficient for capturing fluctuations in renewable energy availability [43]. The model uses weather data from SARAH-2 [44] and ERA5 [45] data sets for the representative year 2013. The techno-economic parameters are chosen to align with projected technological and economic advancements for the year 2045 [46], mostly based on data from the Danish Energy Agency [47]. Industrial commodity demands are modeled according to anticipated defossilization pathways (e.g., electrification of glass industry) based on current demands extracted from JRC-IDEES energy balances [48]. Further exogenous defined commodity demands stem from various open source data sets [49–51].

3.2. Scenario definition

To investigate the impact of utilizing electrolyzer waste heat and oxygen on the overall energy supply – both individually and in combination – four scenarios are defined to characterize the use of these two by-products (Table 2). All scenarios represent alternative configurations of a 2045 climate-neutral German energy system.

- *Base.* Hydrogen is produced via electrolysis without any explicit utilization of electrolyzer by-products. Oxygen is vented and waste heat is not connected to any heat network or industrial demand. This scenario serves as the reference for all other scenarios.
- *WH.* Electrolyzer waste heat can be used in district heating networks and for low-temperature industrial process heat (100 to 150 °C) via heat pumps, while oxygen continues to be vented.
- *O_2.* Electrolyzer oxygen can substitute oxygen from air separation units in conventional applications and enable additional pure-oxygen processes (e.g., oxy-fuel combustion, pure oxygen wastewater treatment), while waste heat is not utilized.
- *Hybrid.* Both waste heat and oxygen from electrolysis can be utilized simultaneously, combining the options from WH and O_2.

Table 2
Scenario overview.

Scenario	Waste heat utilization	Oxygen utilization
Base		
WH	✓	
O_2		✓
Hybrid	✓	✓

All four scenarios share the same boundary conditions, as defined in Section 3.1. Each scenario follows a greenfield approach (cf. Section 2.1 for details on the model), representing a complete new construction of the entire energy system. Thus, the scenarios do not depict a chronological transition pathway but instead represent end-state configurations. This allows for a clear comparison of how enabling different by-product utilization options alters the cost-optimal system design.

4. Results and discussion

The presentation of the results is structured in two main parts: an infrastructure assessment (Section 4.1) and an economic assessment (Section 4.2). These are followed by a consolidated synergy assessment in Section 4.3 and an overarching discussion in Section 4.4.

4.1. Infrastructure assessment

This section begins with a system-level assessment of installed capacities for electrolyzers, ASUs, and alternative heat supply technologies, along with the corresponding oxygen and heat outputs (Section 4.1.1). Subsequently, the spatial distribution of electrolyzer capacities is examined in greater detail in Section 4.1.2, followed by a focused analysis of waste heat and oxygen supply and utilization in Section 4.1.3 and Section 4.1.4, respectively.

4.1.1. Overall capacities and production

Fig. 4 shows the total capacities of the infrastructures for oxygen and heat supply, alongside the corresponding amounts of oxygen and heat produced.

In the base scenario, national heat demand is 1033 TWh/a. In the WH scenario, the national heat demand increases slightly to 1046 TWh/a. The use of electrolysis waste heat thereby enables new heat applications, as further outlined in Section 4.1.3. The total waste heat generated by electrolyzers in the WH scenario is 75 TWh/a, of which 73 TWh/a can be utilized in heat supply, covering ca. 7% of the total heat demand. Considering the electrolyzer infrastructure, waste heat utilization results in a slight increase in installed electrolyzer capacity from 99 GW_{el} to 101 GW_{el}, accompanied by an equivalent increase in hydrogen and, consequently, waste heat production. Consequently, total installed heat supply capacity increases from 526 GW_{th} to 575 GW_{th}. This expansion is driven by the addition of electrolyzer heat capacity and the storage discharging power needed to buffer fluctuating supply. However, this also indicates that, although waste heat utilization substitutes part of the supplied heat, complementary heat supply technologies are still required in a similar order of magnitude in terms of installed capacity to cover the given heat demand, as further outlined in Section 4.1.3.

The conventional oxygen demand is 7 Mt/a, which is fully supplied by ASUs in the base scenario. Additionally, only a small amount of ca. 0.1 Mt/a emerges as part of the extended oxygen applications, which is supplied by ASUs in the base scenario. In the O_2 scenario, the ASUs capacity and the corresponding oxygen production are reduced, so that they only generate the minimum amount required to meet argon demand. In this case, the produced electrolysis oxygen amounts to ca. 70 Mt/a. Integrating parts of this electrolysis oxygen results in a sharp increase in extended oxygen demand to 38 Mt/a, indicating

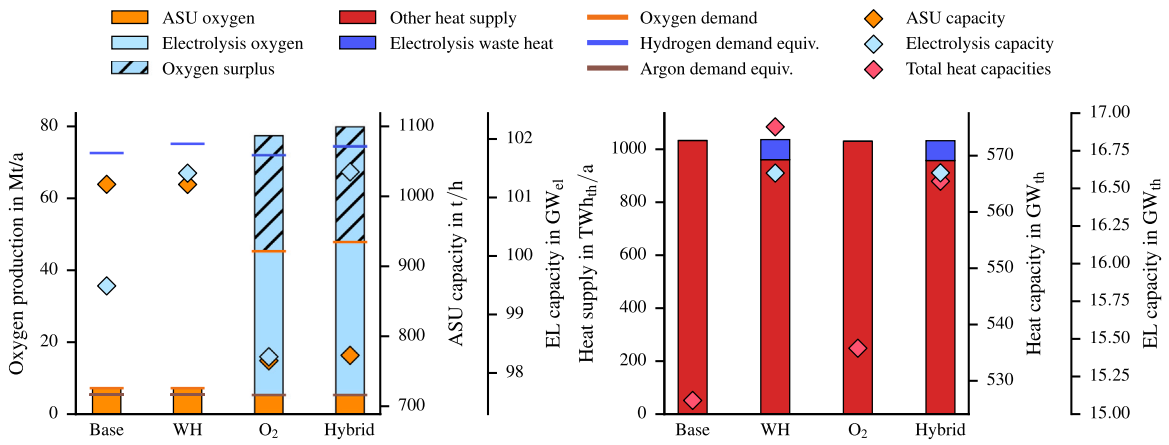

Fig. 4. Overview of by-product related total installed capacities and supplied product amounts across all scenarios. On the left, the total installed capacities of the air separation unit (ASU) and electrolysis (EL), together with the resulting oxygen production, are displayed. In addition, the industrial demands for oxygen, hydrogen, and argon are indicated, as is surplus oxygen from electrolysis. For comparability, hydrogen and argon demand are expressed as equivalent oxygen quantities, representing the amounts that would have been produced by electrolysis and ASUs, respectively. On the right, the total heat supply capacities and the thermal electrolysis capacity ($1\,GW_{el} \approx 0.16\,GW_{th}$), along with the associated (waste) heat supply, are shown.
Source: Adapted from [24].

that low-cost by-product electrolysis oxygen renders new oxygen applications economically viable, as further outlined in Section 4.1.4. Nevertheless, ca. 32 Mt/a of the electrolysis oxygen produced remains unused, suggesting that further utilization potential remains untapped and that full utilization is not economically viable given the assumed current and projected oxygen markets. The fuel and energy savings from extended oxygen applications (as defined in Section 3.1) lead to a slight decrease in system-wide hydrogen demand and, consequently, a reduction in installed electrolyzer capacity to ca. 98 GW_{el}. Total heat demand remains constant, but installed heat supply capacity increases slightly, which is driven by indirect cross-sector effects resulting from changes in fossil fuel use.

In the Hybrid scenario, these individual effects overlap. Compared to the O_2 scenario, the additional waste heat utilization in the Hybrid scenario increases electrolyzer capacity and hydrogen production (as seen in the WH scenario), resulting in installed capacity at the same level as in the WH scenario. The same applies to the remaining heat supply infrastructure, albeit with slightly less storage expansion. However, total hydrogen production, due to oxygen utilization, is slightly lower (as seen in the O_2 scenario). The higher hydrogen production compared to the O_2 scenario also increases oxygen production by 2.5 Mt/a, which is almost entirely utilized. This may result from the development of new sites that become economically viable for oxygen use only through the joint utilization of by-products (cf. Section 4.1.2). This enables additional extended oxygen applications, with synergy effects evident from the combined use of the two electrolysis by-products.

Concluding, the assessment shows that hybrid utilization combines the impacts of individual utilization by enabling conventional supply substitutions, confirming compatibility rather than conflict between utilization pathways.

4.1.2. Spatial capacities

Fig. 5 illustrates the spatially installed electrolyzer capacities on a map of Germany, along with the corresponding local oxygen and heat demand. In the base scenario, electrolyzer capacities are primarily installed in northern Germany due to low electricity procurement costs from wind power generation and the high availability of salt cavern storage facilities. Both waste heat and oxygen utilization influence the choice of location, although the extent of this effect varies depending on the type of by-product:

In the WH scenario, installed electrolyzer capacity tends to shift towards locations characterized by a high heat demand (e.g., Hamburg, Berlin, northwestern Germany), while regions with low heat demand, such as in the northeast, are nearly avoided. However, this redistribution is locally limited and occurs mainly between neighboring regions. Consequently, areas such as the Ruhr region (located in the Midwest of Germany) continue to exhibit low electrolyzer capacity despite the considerable heat demand. Thus, waste heat utilization still reflects a compromise between low electricity procurement costs and high heat integration potential.

In the O_2 scenario, this pattern changes. In contrast to heat utilization, this case shows a stronger supraregional redistribution of electrolyzer capacity. Installation is concentrated around industrial sites with oxygen applications (e.g., Ruhr area, Rhine-Neckar area), leading to the development of regions that were previously neglected.

As already confirmed at the national level in Section 4.1.1, the two individual effects overlap in the Hybrid scenario also on the regional scale. Regions previously avoided due to limited heat utilization potential remain sparsely included, while the spatial convergence of industrial sites (oxygen use) and densely populated areas (waste heat use) persists. These patterns reveal synergy effects between waste heat and oxygen utilization. Industrial sites often exhibit additional high waste heat utilization potential due to process heat and/or high population density in surrounding cities, whereas densely populated regions can provide high oxygen utilization potential through applications such as wastewater treatment. In the Hybrid scenario, these factors drive greater expansion of electrolysis at corresponding locations (e.g., Rhine-Neckar, Federal State of Saxony) compared to the individual scenarios.

A quantitative decomposition of the top 10 electrolyzer nodes (Table B.2) confirms three distinct siting archetypes. First, ‘electricity & storage’ nodes (e.g., 50 in Mecklenburg, 66 in Schleswig-Holstein) dominate the list, serving as baseload hubs driven by access to large-scale salt cavern storage and wind power. Second, ‘synergy’ nodes emerge in industrial clusters; for instance, Saxony (7) and Hamburg (83) host over 7 GW of electrolyzer capacity combined, driven by the coincidence of high oxygen demand and heat loads. Third, specialized nodes like Emsland (82) are driven specifically by industrial oxygen demand, while urban nodes like Berlin (63) are anchored by massive district heating sinks.

The regional analysis reveals distinct redistribution patterns for the individual utilization of each by-product; however, these effects combine under hybrid utilization and, in specific cases of overlap, lead to enhanced outcomes exceeding those of individual use. This confirms that the synergistic effects identified at the national level also

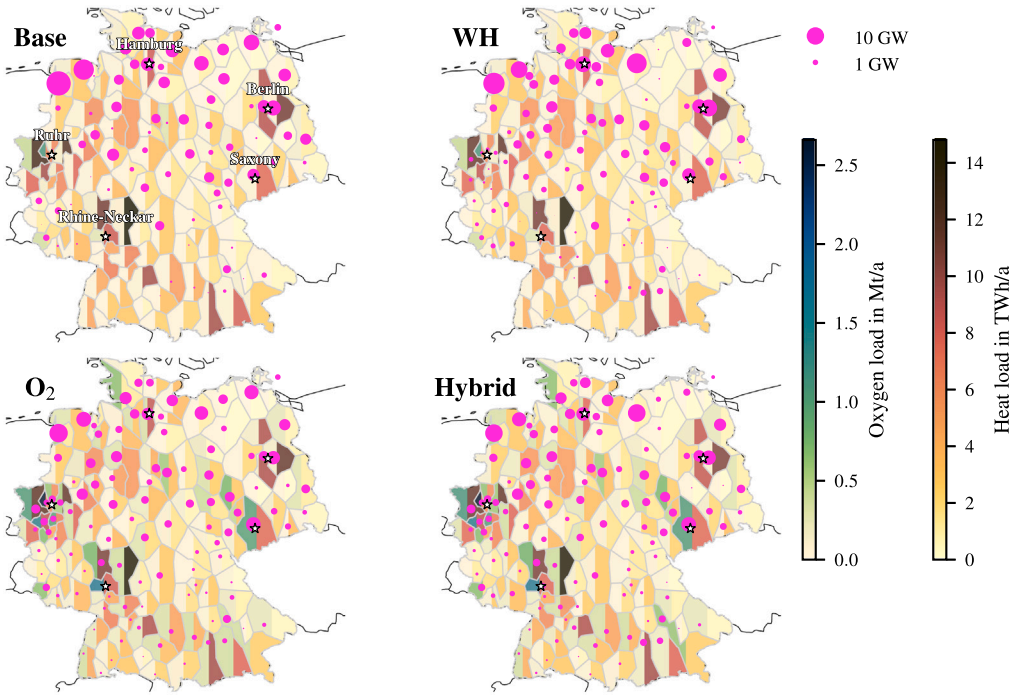

Fig. 5. Spatial distribution of electrolyzer capacities on a map of Germany. Additionally, each region is split vertically and colored according to the local oxygen demand (left half, green/blue) and heat demand (right half, yellow/red).

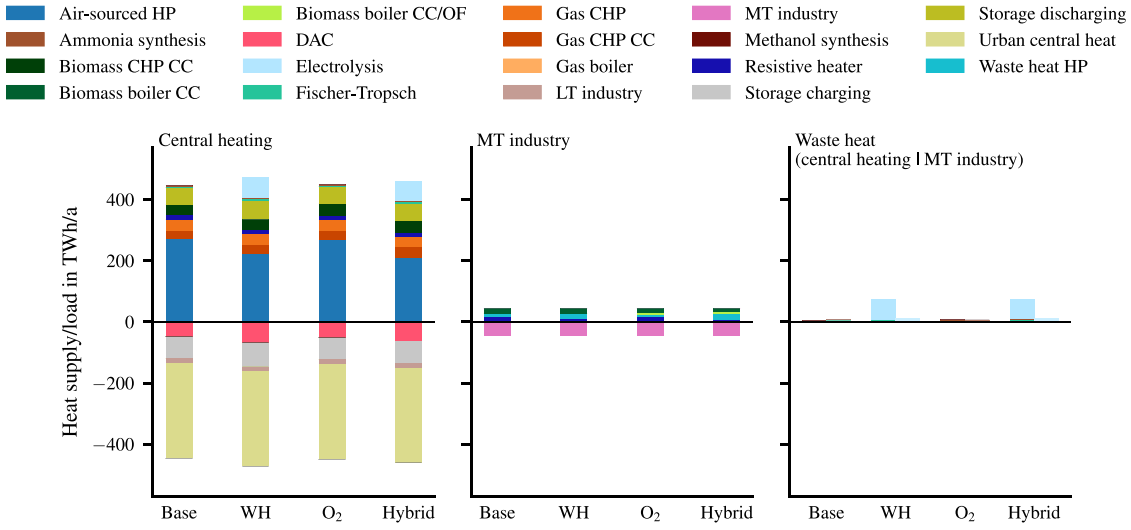

Fig. 6. Balance sheet of heat supply (positive values) and load (negative values) for the heat sectors relevant to electrolysis, namely central heating (left) and mid-temperature (MT) industrial heat (100 to 150 °C, middle), broken down by heat supply technology and heat consumer. Additionally, the provision of waste heat is illustrated (right), divided by the supply to central heating networks and mid-temperature industry (CC: carbon capture, CHP: combined heat and power, DAC: direct air capture, LT: low temperature, HP: heat pump, OF: oxy-fuel).

manifest regionally. Fundamentally, this redistribution reflects a trade-off between maximizing renewable electricity yields and maximizing by-product value. While coastal nodes offer the lowest hydrogen production costs due to high wind availability, the results confirm that the systemic value of local oxygen and heat utilization at inland industrial nodes is sufficient to outweigh the penalty of lower renewable energy availability.

4.1.3. Heat supply

Fig. 6 shows the balance sheet of heat supply and demand for the heat sectors relevant to electrolysis (i.e., central heating, mid-temperature industrial heat, waste heat), broken down by heat supply technology and heat consumer.

In the base scenario, heat supply in central heating networks relies mainly on air-source heat pumps and (synthetic) natural gas and biomass CHP units to meet domestic and low-temperature industrial heat demand and to operate direct air capture systems. The 100 to 150 °C band of mid-temperature industrial heat is supplied equally by biomass boilers, resistive heating, and waste heat-fed heat pumps from Fischer–Tropsch and ammonia synthesis processes.

In the WH scenario, electrolyzer waste heat primarily supplies central heating networks, substituting 18% of the heat supply from air-source heat pumps. Overall, however, heat supply and demand increase in the central heating sector as the utilization of electrolyzer waste heat creates additional heat demand through direct air capture, which

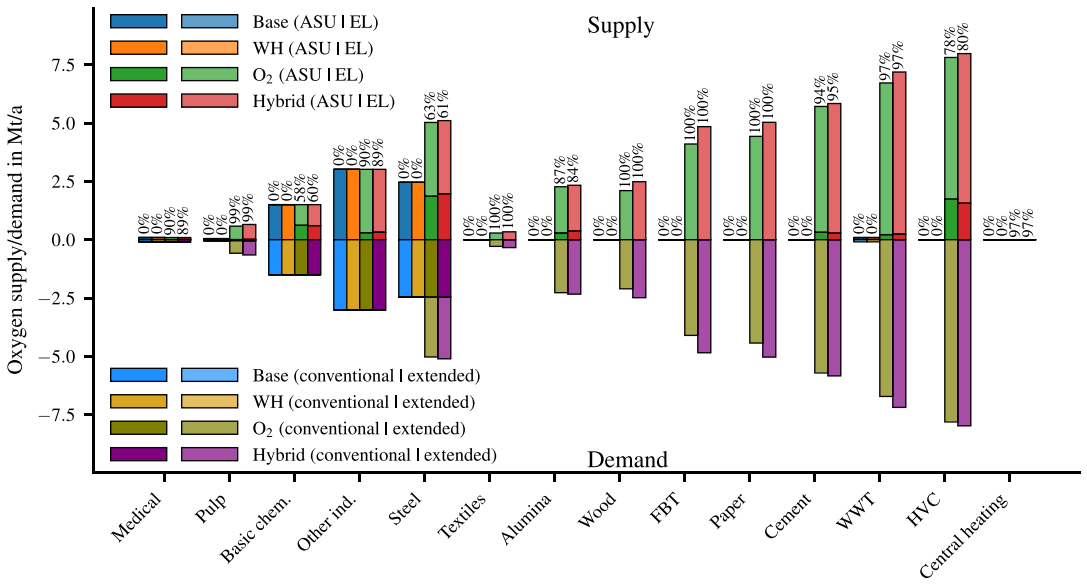

Fig. 7. Oxygen demand – divided into the conventional (i.e., process-related) and extended (i.e., oxy-fuel, wastewater treatment) part – and the corresponding supply from air separation units (ASU) and electrolysis (EL) across all oxygen applications. The supply share from electrolysis is shown above the bars (HVC: high-value chemicals, FBT: food, beverages and tobacco, WWT: wastewater treatment).

rises by ca. 40%. In the mid-temperature industrial heat sector, a minor amount of electrolyzer waste heat is used via waste heat-fed heat pumps (cf. Fig. 2), which replace ca. 40% of the resistive heating supply. As outlined in Section 4.1.1, the utilization of electrolyzer waste heat therefore not only leads to substitution of conventional supply, but also opens up new heat demand beyond the conventional heating sector (i.e., direct air capture).

The O_2 scenario shows no significant impact on central heating. Indirectly, however, there is an impact on mid-temperature industrial heat, as some biomass boilers, including carbon capture systems, are being converted to oxy-fuel combustion. Due to the local availability of inexpensive electrolysis oxygen, it appears economical from an energy system perspective to convert at least a part of industrial heat supply to oxy-fuel processes to achieve higher fuel efficiency and capture rates.

In the Hybrid scenario, similar effects are observed for central heating as in the WH scenario. Only the heat demand for direct air capture is lower (increase of 30%), because more oxy-fuel-based processes, including higher capture rates, are utilized across the energy system, thus reducing the need for additional direct air capture. This reveals a mutually restrictive effect of the joint by-product utilization potentials, which is also reflected in a slightly lower waste heat utilization share of 97.1% compared to 97.5% as in the WH scenario. The increased expansion of electrolyzer capacity at industrial sites with concurrent oxygen and heat demands (cf. Section 4.1.2 for spatial concurrence of electrolyzer capacities and by-product demand) leads to a larger share of oxy-fuel-based biomass boilers and heat pumps supplied with electrolyzer waste heat in the mid-temperature industrial heat sector.

The results illustrate the effects on conventional heat supply infrastructure, not only by substituting parts of conventional supply options but also by generating additional demand. In this context, however, the combined utilization of by-products exhibits a minor limiting effect, as the increased application of oxy-fuel combustion enabled by oxygen utilization indirectly reduces heat demand and thereby slightly decreases the utilization potential of electrolysis waste heat. Furthermore, the substitution effects remain relatively small, indicating that most conventional supply capacities must be maintained. Crucially, the results indicate that this waste heat does not primarily displace fossil-based heat supply but instead substitutes air-source heat pumps. While this mechanism does not result in direct defossilization, it reduces overall electricity demand for heat provision, which in turn indirectly supports defossilization by freeing renewable electricity for use in other sectors or by lowering the overall demand for renewable generation capacity.

4.1.4. Oxygen supply

Fig. 7 shows the oxygen supply by ASUs and electrolyzers across all considered industrial oxygen applications, broken down into conventional (i.e., process-related) and extended (i.e., oxy-fuel, wastewater treatment) demand.

In the scenarios without electrolysis oxygen utilization (base, WH), the entire oxygen demand is supplied by ASUs. This demand consists predominantly of the process-related conventional demand, while only a very small amount of extended oxygen is used in wastewater treatment. This indicates that extended applications supplied by oxygen from ASUs are generally too costly and therefore not economically competitive.

However, the prevalence of these applications changes with the utilization of electrolysis oxygen (O_2, Hybrid scenarios). In the O_2 scenario, a sharp increase in oxygen demand is observed due to extended applications, particularly in the steel and HVC industries as well as in wastewater treatment. Therefore, the utilization of electrolysis oxygen enables several industrial applications in which pure oxygen was not previously used (i.e., HVC, cement, alumina, paper, FBT, wood, wastewater treatment). The application in CHPs within the central heating sector is negligible. This suggests that improved capture rates alone are insufficient to ensure the economic viability of oxy-fuel processes within the central heating sector.

Some oxy-fuel processes are supplied with oxygen from ASUs (i.e., steel, HVC, alumina). This is driven by the requirement to supply argon, which entails a minimum level of oxygen production from ASUs to cover the given argon demand. Accordingly, ASUs are mainly located near major industrial oxygen consumers to complement and balance the fluctuating oxygen supply from electrolyzers.

The increase in oxygen demand in the Hybrid scenario compared to the O_2 scenario illustrates the synergy effect of simultaneous by-product utilization. Waste heat utilization promotes a slight increase in hydrogen production, which is accompanied by an increase in oxygen production, as detailed in Section 4.1.1. However, this increase does not result in additional surplus oxygen but can be used to expand oxy-fuel and wastewater treatment applications relative to the O_2 scenario.

In summary, similar to waste heat utilization, oxygen utilization leads to a partial substitution of conventional infrastructure and a considerable increase in new oxygen demand driven by entirely new

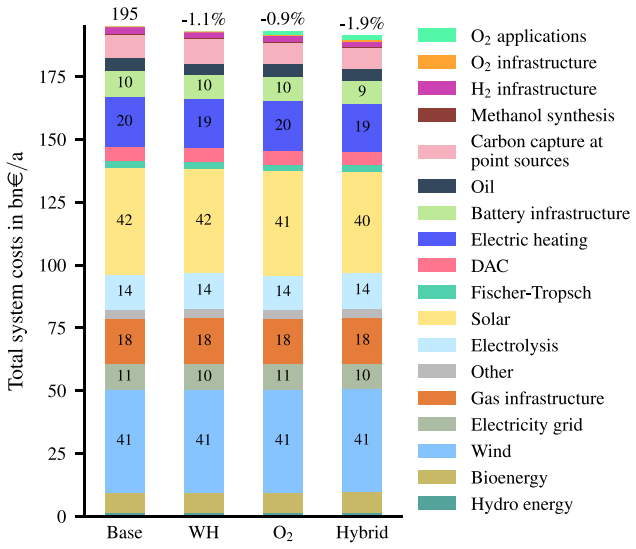

Fig. 8. Total annual costs of the entire energy system, broken down by technology group. 'Gas infrastructure' and 'Bioenergy' include all methane- and biomass-based combustion technologies without carbon capture. All remaining combustion technologies with carbon capture are grouped under 'Carbon capture at point sources', except for those based on oxy-fuel, which are classified as 'O_2 applications'. 'H_2 infrastructure' mainly includes pipelines and storage (DAC: direct air capture, WH: waste heat, visualization adapted from [33]).

applications, indicating investment opportunities in emerging oxygen-based processes. The combined utilization of both by-products, however, demonstrates a predominantly synergistic effect, as the additional quantities of oxygen produced from electrolysis can largely be integrated in an economically viable manner.

4.2. Economic assessment

The following section presents the economic evaluation of the utilization of electrolyzer by-products. This assessment is first conducted from a systemic perspective based on the total annual costs of the entire energy system in Section 4.2.1, followed by a focus on hydrogen production using the LCOH in Section 4.2.2.

4.2.1. Total costs

Fig. 8 shows the total annual costs of the considered German energy system, broken down by the contributions of the respective technology groups. In the base scenario, the total annual costs amount to 195 bn€/a. The WH scenario reduces these costs by 1.1%, primarily due to savings in electrical heat supply and reduced necessity for related battery infrastructure. The O_2 scenario reduces the total annual costs by 0.9%, mainly through savings in solar energy generation, direct air capture, and carbon capture without oxy-fuel; effects that can be attributed to efficiency gains and improved industrial carbon capture rates resulting from the wider application of oxy-fuel processes and wastewater treatment with electrolysis oxygen.

The Hybrid scenario yields cost savings of 1.9%, representing an almost perfectly additive combination of the individual benefits. That the savings in the Hybrid scenario closely match the sum of the savings from the individual scenarios indicates that oxygen and waste heat utilization act through largely independent economic mechanisms. Consequently, the joint utilization of electrolyzer by-products generates synergistic effects, with only limited interference between the respective individual savings potentials.

A more detailed breakdown of the total annual system cost changes for each technology group, normalized by the respective hydrogen production, is provided in Fig. B.1.

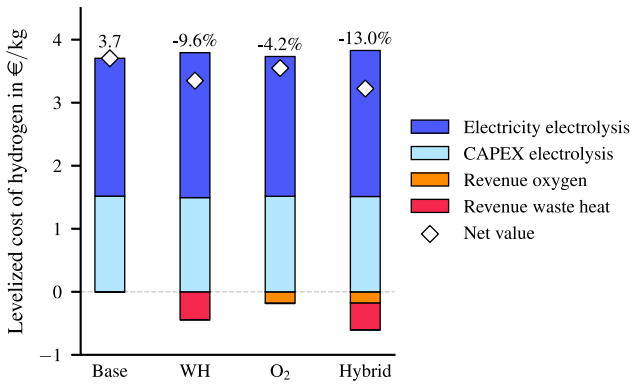

Fig. 9. Average national levelized cost of hydrogen, broken down by cost elements (WH: waste heat).

4.2.2. Levelized cost of hydrogen

Within this section, the LCOH are presented as nation-wide and spatial averages.

National levelized cost of hydrogen. Fig. 9 illustrates the average national LCOH. In the base scenario, the LCOH amounts to 3.7 €/kg, driven primarily by the investment costs of the electrolyzers and their operating electricity costs. The contribution of electrolyzer investment costs remains largely constant across the scenarios (i.e., ca. 1.5 €/kg) and is therefore not further discussed in the following. By contrast, revenues from by-product commercialization vary considerably between scenarios.

The WH scenario reduces LCOH by 9.6% to ca. 3.3 €/kg. Although the sale of waste heat generates revenues of ca. 0.44 €/kg, the share of electricity costs also increases by ca. 0.1 €/kg. This cost increase stems from three factors: a deviation from optimal siting compared to the base scenario, higher overall electrolyzer deployment, and less cost-effective dispatch. To align hydrogen production with heat demand, electrolyzers must operate at times with less favorable electricity prices.

The O_2 scenario reduces LCOH by 4.2% to ca. 3.5 €/kg. At ca. 0.18 €/kg, revenues from oxygen sales are lower than those from waste heat, but the share of electricity costs rises less. The lower oxygen revenues are attributable to two factors. First, unlike waste heat, only about 55% of the total oxygen produced is actually integrated, limiting revenue potential relative to the total hydrogen output. Second, surplus electrolysis oxygen depresses marginal oxygen prices – particularly in northern Germany – further reducing revenues. The less pronounced increase in electricity costs is partly explained by a greater use of southern sites, where low-cost photovoltaic (PV) electricity can be utilized to a limited extent – unlike in the WH scenario, which relies less on these locations (Fig. 10).

The Hybrid scenario achieves the greatest savings, with the LCOH decreasing by 13% to ca. 3.2 €/kg. The individual cost reductions achieved in the separate scenarios are not fully reproduced in the combined case. Revenues from waste heat and oxygen sales fall slightly compared to the individual scenarios, while electricity procurement costs account for the largest share among all scenarios. Consequently, joint utilization tends to require greater compromises in the utilization potential of by-products compared to individual utilization, and to exploit this potential as fully as possible, even more locations with less favorable electricity procurement costs are selected.

Nevertheless, only minor concessions are required in terms of savings, indicating that synergy effects outweigh the mutual restrictions in joint utilization and that these synergy effects – already observed from an infrastructural perspective – are also reflected in the LCOH. Compared to the total costs, however, waste heat utilization provides greater direct economic benefits for electrolyzer operators, whereas oxygen utilization unfolds its advantages primarily at the energy system level through indirect effects that are not fully captured by market prices within the LCOH framework.

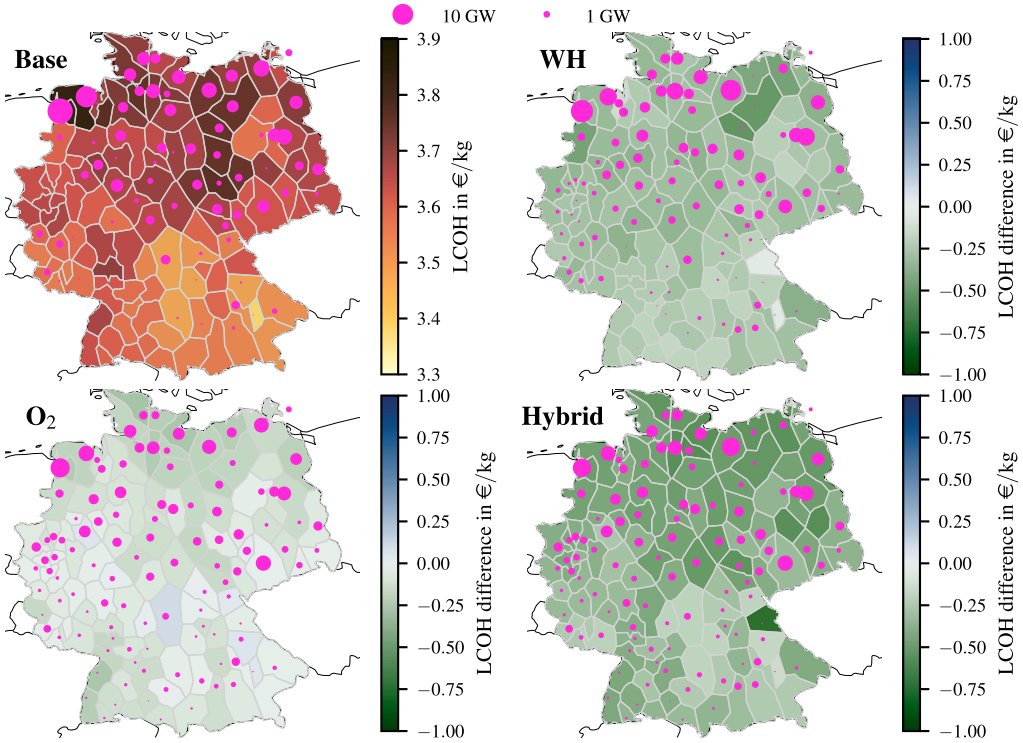

Fig. 10. Spatial distribution of electrolyzer capacities on a map of Germany. For the base scenario, each region is colored according to the local annual average levelized cost of hydrogen (LCOH), while for the remaining scenarios, the absolute difference compared to the base scenario is shown.

Spatial levelized cost of hydrogen. In addition to the average national LCOH, the spatial distribution of average LCOH is shown in Fig. 10. In the base scenario, southern Germany exhibit lower LCOH than the rest of the country, despite significantly lower electrolyzer deployment. This can be explained by two factors. First, electrolyzers are primarily sited near salt caverns that allow for hydrogen storage, which are predominantly located in central and northern Germany. Second, large-scale electrolyzer deployment relies on large-scale electricity supply, which is more readily available from wind expansion in northern Germany than from PV expansion in the south. Nonetheless, the lower electricity costs from PV in southern Germany enable smaller electrolyzers to benefit from this profile and produce hydrogen at comparatively lower LCOH.

In the WH scenario, LCOH reduction is observed across almost all of Germany, indicating that nearly every region benefits from waste heat utilization. In contrast, oxygen utilization (O_2 scenario) exhibits a much more selective spatial distribution and a smaller absolute reduction in LCOH, as shown in Fig. 9. Since spatial demand for oxygen is less widespread than for heat, only specific regions (i.e., industrial sites) benefit from oxygen utilization. To realize these system-level benefits, however, LCOH slightly increase in certain regions (e.g., central and southeast Germany) due to higher electrolyzer capacities, highlighting that in southern Germany it is only possible to exploit low-cost PV electricity to a limited extent as in the base case.

The joint utilization of by-products (Hybrid scenario) again reveals a complementarity of the two individual effects. While LCOH reductions can be achieved in almost every region, the magnitude of the potential savings varies more strongly than in the individual scenarios. For example, reductions of ca. 0.25 €/kg occur in the region around Berlin, whereas reductions of up to 0.6 €/kg are possible in parts of central and northern Germany. In one region in southern Germany, LCOH decrease by 0.8 €/kg. However, this region is characterized by very limited electrolysis capacities, so even minor absolute changes translate into disproportionately large relative improvements without contributing significantly to the overall system context.

Overall, similar to the total annual cost (cf. Section 4.2.1), the analysis indicates that the individual cost reductions achieved through joint utilization are nearly additive and that this approach is advantageous from an electrolyzer operator's perspective across most regions in Germany, although the absolute savings potential is highly location-dependent and varies considerably between regions. However, the results also reveal a critical divergence between system-level benefits and operator-level revenues: while oxygen utilization yields system cost savings of 0.9%, comparable to waste heat's 1.1%, its associated LCOH reduction amounts to only 4.2% compared to 9.6% for waste heat. This indicates that the underlying market mechanisms insufficiently incentivize oxygen utilization despite its substantial cross-sectoral benefits. This market inefficiency – driven by surplus oxygen depressing marginal prices and by limited utilization potential – highlights the need for targeted policy interventions (e.g., oxygen production subsidies or oxy-fuel retrofit incentives) to better align private investment decisions with system-optimal outcomes. These aspects are further discussed in Section 4.4.

4.3. Assessment summary

To conclude the results regarding synergies in by-product utilization, Table 3 summarizes the key metrics discussed above. From both a total system perspective (TAC) and an electrolyzer operator perspective (LCOH), the synergy index – as the ratio of joint utilization outcomes to the superpositioned outcomes of isolated utilization – range between 0.94 and 0.95. These values indicate effects that are nearly additive, implying that joint utilization entails hardly any mutual constraints and that economic benefits are largely preserved, when both by-products are used simultaneously.

A similar pattern emerges for the share of waste heat utilized relative to total waste heat produced. Here, the synergy index is slightly subadditive at around 0.99, but the deviation is negligible, indicating no meaningful limitation due to joint utilization. For oxygen utilization, the synergy index even exceeds unity, reaching 1.06, which points to a superadditive effect and thus a clear synergy.

Overall, the utilization pathways of the two by-products hardly constrain each other. Instead, they exhibit predominantly synergistic interactions, reinforcing the value of combined by-product utilization.

Table 3
Comparison of key metrics across scenarios and quantitative synergy of the Hybrid scenario. 'WH+O_2' indicates the expected value by superposition of the WH and O_2 results. The synergy index expresses the relation of the Hybrid to the 'WH+O_2' result. Waste heat and O_2 share represents the quote of utilized by-product in relation to the total amount produced (WH: waste heat, TAC: total annualized cost, LCOH: levelized cost of hydrogen).

Metric	Unit	Base	WH	O_2	WH+O_2	Hybrid	Synergy
TAC	bn€/a	195.0	192.9	193.1	191.0	191.3	
TAC change vs. base	%	0.0	−1.1	−0.9	−2.0	−1.9	0.95
Avg. LCOH	€/kg	3.70	3.35	3.54	3.19	3.22	
LCOH change vs. base	%	0.0	−9.6	−4.2	−13.8	−13.0	0.94
Utilized waste heat	TWh/a	0	73.9	0	73.9	72.8	0.99
Utilized waste heat share	%	0	97.5	0	97.5	97.1	0.996
Utilized O_2	Mt/a	0	0	39.8	39.8	42.3	1.06
Utilized O_2 share	%	0	0	55	55	57	1.04

4.4. Overall discussion

This study examines combined oxygen and waste heat utilization within a spatially resolved German energy system, addressing four research gaps. First, joint by-product utilization achieves near-perfect additive cost savings by reducing total annual system costs by 1.9% versus 2.0% expected from overlying of individual pathways (Table 3). This demonstrates that oxygen and waste heat utilization operates through rather independent economic pathways on the system-level. Within the energy system, waste heat utilization primarily substitutes other heat supply technologies directly, whereas oxygen utilization exerts a more indirect influence by partially replacing ASU capacities and, more importantly, enabling new or converted industrial processes (e.g., oxy-fuel combustion, wastewater treatment), which subsequently affect other sectors.

Second, both utilization pathways are economically equally relevant at the energy system level (i.e., total annual system costs) but not on the operator-level (i.e., LCOH). Although both options yield substantial savings, the effect of waste heat utilization (9.6%) on reducing LCOH is significantly greater than that of oxygen utilization (4.2%). This indicates that the rather indirect benefits from oxygen utilization are not adequately reflected in the market price of oxygen – further exaggerated due to substantial surplus oxygen from electrolyzers that depresses prices – limiting the visibility of these benefits to operators in the form of sales revenues. To nevertheless leverage these positive system effects, such price differentials could potentially be compensated through targeted incentives, thereby motivating oxygen utilization by electrolyzer operators.

Third, the utilization of electrolysis by-products significantly influences the cost-optimal spatial allocation and integration of electrolyzers within the overall energy system. Without by-product utilization, electrolyzers concentrate in northern Germany, driven by low-cost renewable electricity and the availability of salt cavern storage. In contrast, waste heat utilization shifts capacities towards heat demand centers like Hamburg and Berlin. Similarly, oxygen utilization directs siting towards major industrial hubs, such as the Ruhr and Rhine-Neckar regions to maximize utilization potential. In both cases, however, a balance must be maintained between utilization potential, and local electricity procurement costs and supply, preventing arbitrary redistribution of installed capacities. Waste heat utilization predominantly results in redistribution between neighboring regions, whereas oxygen utilization also opens opportunities in more distant areas, as the conversion of industrial processes to pure oxygen applications (e.g., oxy-fuel combustion) yields considerable benefits from an energy system perspective, outweighing less-favorable electricity costs and longer distance to salt cavern storage. Through joint utilization, these effects are further strengthened and new sites emerge that would not be economically viable through the use of only one by-product, highlighting the necessity of forward-looking planning that incorporates the joint utilization of both by-products to fully realize synergy effects.

Fourth, the utilization of both electrolyzer by-products leads to the substitution of conventional supply while simultaneously increasing the overall demand for each product. Waste heat utilization primarily replaces heat previously provided by air-source heat pumps and slightly increases total heat demand, as a greater number of direct air capture units is supplied via central heating networks. Oxygen utilization partly substitutes oxygen from ASUs while also creating substantial new demand, since the availability of electrolyzer oxygen makes some of the considered pure oxygen-based industrial processes economically viable. However, the integration of oxygen into new industrial processes slightly limits the potential for waste heat utilization, as it indirectly reduces system-wide heat demand – particularly from DAC plants. Conversely, waste heat utilization is associated with a modest increase in hydrogen production, and thus in oxygen generation, with this additional oxygen volume being economically integrated into the system. Therefore, the interaction between both utilization pathways is asymmetric: while oxygen utilization modestly constrains the potential for waste heat utilization, waste heat utilization does not impose a corresponding limitation on oxygen utilization.

4.4.1. Comparison with literature

Levelized cost and utilization rates. In the literature, LCOH reductions achieved through waste heat utilization are reported in the range of 0.1 to 0.3 €/kg [18,19,26,29]. In this study, the national average absolute reduction amounts to 0.4 €/kg, which slightly exceeds the values reported in the literature.

For oxygen utilization, literature sources indicate LCOH reductions between 0.2 to 0.9 €/kg [16,21,23,24]. The results of this study show a national average reduction of 0.2 €/kg, placing the absolute reduction at the lower end of the reported range. Overall, the national average LCOH reductions obtained in this study are broadly consistent with previous findings.

The spatially high-resolution modeling approach applied in this study further enables the assessment of LCOH reductions for each individual node. For waste heat utilization, the range spans from 0.06 to 0.56 €/kg; for oxygen utilization, from −0.11 to 0.29 €/kg; and for hybrid utilization, from 0.16 to 0.79 €/kg. These results demonstrate that, while the national average provides a useful indication of overall cost reduction potential, the effects are highly location-dependent. In the case of oxygen utilization, system-optimal integration may even result in higher LCOH, leading to disadvantages from an operator perspective. In contrast, joint utilization ensures cost reductions across all locations. By accounting for diverse regional conditions, the approach taken in this study enables more robust conclusions on cost reduction potentials compared to previous analyses that often focus on a single site with fixed boundary conditions.

Furthermore, by-product sale revenues in this study are derived from the resulting marginal prices for oxygen and waste heat, providing a market-based representation, whereas prior studies typically assume fixed by-product prices. The higher absolute reductions achieved through waste heat utilization suggest that earlier studies likely assumed more conservative waste heat prices and/or lower utilization potentials for electrolyzer waste heat. In the Hybrid scenario, this study identifies an utilization potential of 97%, compared to the 85

to 90% typically reported in the literature [19]. When examining the nodal utilization rates, values range from 59 to 99.8%. The low values, however, represent isolated outliers, as the median utilization amounts to 99.0%.

Conversely, the lower absolute reductions observed for oxygen utilization indicate that prior studies may have assumed overly optimistic oxygen prices and utilization levels. In this study, in the Hybrid scenario, only about 55% of the total oxygen produced from electrolyzers can be utilized economically, while the remaining surplus further suppresses oxygen market prices. However, a site-specific assessment remains essential, as the local utilization rate varies substantially between 8 to 75% at the nodal level. At the same time, the results show that locally produced oxygen cannot be fully absorbed in any region.

Waste heat applications. The results of this study indicate that most electrolyzer waste heat is used for low-temperature applications in district heating networks rather than for medium-temperature industrial processes. This finding contrasts with [26], which identifies utilization via heat pumps as the more economically favorable option. The difference arises because the present study also accounts for biomass-based heat supply, which, particularly when combined with carbon capture, provides additional value beyond mere heat provision. Consequently, a portion of medium-temperature industrial heat is supplied through biomass combustion, resulting in a higher potential for direct utilization of electrolyzer waste heat in low-temperature rather then medium-temperature applications.

Spatial redistribution. The qualitative findings from our previous study based on isolated oxygen utilization are confirmed [24]. That study also demonstrated that electrolyzers are increasingly sited according to local oxygen demand. The new insight, however, is that similar redistribution patterns emerge for waste heat utilization – although to a somewhat lesser extent spatially – and that both effects complement each other in the case of joint by-product utilization. Certain locations become economically viable for bigger-scale hydrogen production only when both by-products are utilized simultaneously.

4.4.2. Implications

The German National Hydrogen Strategy explicitly states that the potential for electrolyzer waste heat utilization should be considered when selecting electrolyzer sites, alongside factors such as renewable electricity availability and electricity grid constraints [52]. The findings of this study reinforce this point: strategically locating electrolyzers near industrial and urban areas to facilitate by-product utilization enables notable cost reductions, both at the total system level and from the perspective of electrolyzer operators.

These cost reductions in hydrogen production also support hydrogen targets at the European level. The REPowerEU plan aims for 10 Mt/a of domestic renewable hydrogen production by 2030, yet a persistent challenge is the cost gap relative to imported hydrogen [53]. This study shows that combined utilization of electrolyzer by-products can reduce the LCOH of domestically produced hydrogen by approximately 13%. Importantly, these cost reductions are realized without assuming further technological breakthroughs in electrolyzers themselves; instead, they arise from improved integration with heat, oxygen, and CO_2 management infrastructure.

This indicates that part of the cost gap between domestic production and imports, often highlighted in the REPowerEU discussion, can be mitigated through enhanced system-integration measures. Consequently, the results support REPowerEU's objective of enabling a cost-effective scale-up of renewable hydrogen in Europe [53].

However, realizing these potentials requires extensive modifications to the existing energy infrastructure for large-scale implementation (e.g., retrofitting or constructing industrial heat supply systems compatible with oxy-fuel combustion, developing local oxygen and heat networks to facilitate by-product utilization). Such measures would affect not only stakeholders directly involved in electrolyzer deployment but also actors in adjacent sectors (e.g., heating, industry), thereby necessitating coordinated and cross-sectoral efforts. Moreover, these transformations require sufficient certainty for both consumers and electrolyzer operators regarding purchase volumes and economic conditions to ensure long-term investment security.

Joint by-product utilization can help address these challenges by achieving the greatest LCOH reduction and diversifying revenues across two commodities, thus improving economic resilience. However, since the cost-optimal solutions identified in this study differ in some cases substantially from those without by-product utilization (e.g., in terms of site selection), real-world implementation carries risks associated with reliance on sufficient by-product uptake to sustain competitiveness. This reflects a fundamental challenge for by-product utilization: the location of electrolyzers plays a decisive role in realizing the potential benefits of by-product utilization and must therefore be considered early in infrastructure planning to prevent future lock-in effects.

At the same time, the results, particularly regarding oxygen utilization, highlight that new sources of high oxygen demand must first emerge to make oxygen utilization economically viable from the perspective of electrolyzer operators. However, these new oxygen-based applications only become economically feasible once sufficient low-cost electrolysis oxygen is available. This interdependence creates a classic chicken-and-egg problem, emphasizing the need for coordinated, cross-sector infrastructure planning.

Targeted policy measures could play a decisive role in reducing the risks associated with electrolyzer siting redistribution and in enabling the economically efficient utilization of by-products. To stimulate sufficient demand, retrofit support schemes may be introduced for both district heating networks and oxy-fuel industrial processes. In addition, pricing mechanisms that guarantee a minimum purchase price for electrolyzer oxygen – even under conditions of oversupply – could enhance economic certainty for electrolyzer operators. Further, operators could be granted reduced grid fees if they demonstrate by-product utilization alongside hydrogen production, thereby creating an additional incentive to locate within industrial clusters. Overall, such measures would help align private investment incentives with system-optimal outcomes and facilitate a cost-effective transformation of the energy system.

4.4.3. Limitations and outlook

The model approach used in this study is applied to the German energy system, but it can also be universally applied to other European countries or the entire European energy system. This study deliberately focused solely on the German energy system in order to be able to use a high spatial resolution at a reasonable computational cost, which is necessary to map the potential spatial mismatch between the availability of sufficient electricity from renewable energies and the demand for by-products. In this case, imports of fossil fuels were taken into account for the isolated German energy system, but not imports of hydrogen. Consequently, the entire hydrogen demand is assumed to be met through domestic production, which may lead to an overestimation of German electrolyzer capacity requirements. Nonetheless, total capacities in the model are around 100 GW, with annual production of ca. 300 TWh/a. For 2045, a domestic production of 190 to 245 TWh/a and domestic capacities of 80 to 100 GW [52] are projected, placing the results within a reasonable range.

This effect is also influenced by the assumed carbon capture and storage (CCS) budget. A sensitivity analysis indicates that tighter CCS limits lead to increased reliance on "green" hydrogen, thereby raising electrolyzer capacity and the associated hydrogen production (Table B.1). Nevertheless, across the range of CCS assumptions, the achievable LCOH reductions remain within a similar band of 11.9 to 13.4% (13.0% for a CCS budget of 100 Mt/a). In terms of total annual system costs, the savings are even more pronounced, reaching 2.6% compared to 1.9%, as oxy-fuel combustion is even more beneficial under more restrictive CCS budgets due to the higher capture rates and improved fuel efficiency. Overall, these results indicate that the findings of this study remain

robust even if the CCS budget available to Germany in the future is lower than assumed.

While backbone infrastructure (e.g., electricity grid, hydrogen pipelines) is fully costed, the model simplifies local utilization. Specifically, the CAPEX for short-distance waste heat connections and oxygen distribution manifolds within industrial parks is assumed to be part of the general installation costs. However, in the case of oxygen, this is the same for ASUs and electrolyzers, so the baseline for relative costs reductions is the same. Nonetheless, including detailed brownfield retrofit engineering costs would likely reduce the (absolute) net economic benefit, though without altering the qualitative finding that by-product utilization drives system-optimal siting towards industrial clusters.

Future work could apply this approach to other European countries to investigate whether the findings from Germany can also be transferred to other, possibly less industrialized countries, or examine the entire European energy system to see whether a redistribution of electrolyzer locations can also be observed in this case, or whether this is not economically viable due to cross-border hydrogen transport. In addition, other technologies for by-product utilization, such as the Allam Cycle process for pure oxygen utilization, could be implemented to further utilize by-product surpluses.

5. Summary

Hydrogen is considered a key energy carrier for comprehensive defossilization of energy systems. However, large-scale deployment of "green" hydrogen production via electrolyzers powered by renewable energy sources faces significant cost barriers. One promising approach to address this challenge is the utilization of by-products – oxygen and waste heat – generated during electrolyzer operation. Since no previous study has examined the combined utilization of these two by-products within a spatially explicit energy system framework, this study addresses this research gap by answering questions regarding the synergistic effects, market mechanism effectiveness, electrolyzer siting implications, and conventional infrastructure substitution potential of combined oxygen and waste heat utilization. These research questions are investigated through co-optimization of design and operation of the German energy system across five interconnected sectors (i.e., electricity, heating, industry, transport, biomass) using high-granular spatial resolution. The main results can be summarized as follows.

- Joint waste heat and oxygen by-product utilization delivers substantial economic benefits: 1.9% reduction in total annual system costs (3.7 bn€/a) and 13% reduction in LCOH. These savings demonstrate near-perfect additivity, as individual reduction contributions from waste heat (1.1% system costs, 9.6% LCOH) and oxygen (0.9% system costs, 4.2% LCOH) are almost fully captured in combined utilization, confirming synergistic rather than competing effects.
- Both by-products provide comparable system-level cost reductions (1.1% vs 0.9%) but diverge substantially in operator-level benefits: waste heat achieves 9.6% LCOH reduction versus oxygen's 4.2%. This asymmetry reveals market failure where oxygen's indirect benefits (improved carbon capture rates, fuel efficiency gains, enabled wastewater treatment) accrue to industrial consumers rather than hydrogen producers, while surplus electrolyzer oxygen depresses market prices, limiting operator revenue capture despite substantial system-level value creation.
- By-product utilization fundamentally alters cost-optimal electrolyzer siting. Without by-products, capacity concentrates in northern Germany due to low-cost renewable electricity and salt cavern availability. Waste heat utilization shifts capacity towards high-demand regions through rather short-distance redistribution between neighboring areas. Oxygen utilization enables supraregional capacity shifts to industrial hubs, where oxy-fuel conversion benefits outweigh less-favorable electricity costs and greater distances to storage. Combined by-product utilization strengthens these effects and unlocks synergy sites where co-located oxygen and heat demands enable economically viable electrolyzer deployment that would be infeasible with single by-product utilization alone, highlighting the necessity of integrated planning to capture full synergy potential.
- By-product utilization both partly substitutes conventional supply and increases overall demand. Waste heat primarily replaces air-source heat pumps while modestly increasing total heat demand through additional direct air capture units supplied via central heating networks. Oxygen partially substitutes ASUs while creating substantial new demand by rendering pure oxygen-based industrial processes economically viable. The interaction between utilization pathways is asymmetric: oxygen utilization modestly constrains waste heat potential by reducing system-wide heat demand (particularly from direct air capture), whereas waste heat utilization increases hydrogen production and thus oxygen generation, with this additional oxygen being economically integrated. Consequently, waste heat utilization does not limit oxygen utilization, revealing a unidirectional constraint rather than mutual interference. Nevertheless, in both cases, significant capacities of conventional supply technologies have to be maintained.
- Exploiting these benefits requires additional cross-sector infrastructure measures. For oxygen utilization, some industrial processes would need to be adapted to oxygen-based applications (e.g., oxy-fuel combustion). For waste heat utilization, the expansion of local heating networks and the deployment of waste heat-fed heat pumps would be necessary to integrate the waste heat from electrolysis.

This study provides a comprehensive, spatially explicit analysis of combined electrolyzer by-product utilization, demonstrating that joint oxygen and waste heat utilization can reduce hydrogen production costs by 13% while simultaneously improving overall energy system efficiency. The high spatial resolution enables precise identification of synergy hotspots at industrial-urban sites and infrastructure transition pathways, providing actionable guidance for regional electrolyzer deployment strategies. While Germany serves as the case study, the optimization modeling framework is transferable to other European countries. The findings provide insights for policymakers, infrastructure planners, and electrolyzer operators facing imminent investment decisions, demonstrating that by-product utilization represents not merely an optimization of hydrogen economics but a fundamental restructuring of energy system architecture requiring integrated planning from project inception to fully capture economic and efficiency benefits towards 2050 climate neutrality targets.

CRediT authorship contribution statement

Luka Bornemann: Writing – original draft, Software, Methodology, Formal analysis, Data curation, Conceptualization. **Wolfram Tuschewitzki:** Writing – review & editing, Conceptualization. **Martin Kaltschmitt:** Writing – review & editing, Supervision, Funding acquisition, Conceptualization.

Declaration of Generative AI and AI-assisted technologies in the writing process

During the preparation of this work the authors used ChatGPT in order to improve readability and language. After using this tool/service, the authors reviewed and edited the content as needed and take full responsibility for the content of the publication.

Declaration of competing interest

The authors declare that they have no known competing financial interests or personal relationships that could have appeared to influence the work reported in this paper.

Acknowledgments

This work is funded by dtec.bw – Digitalization and Technology Research Center of the Bundeswehr. The support is gratefully acknowledged. dtec.bw is funded by the European Union – NextGenerationEU. Publishing fees supported by Funding Programme Open Access Publishing of Hamburg University of Technology (TUHH).

Appendix A. Energy system model

A.1. General mathematical formulation

This section summarizes the mathematical formulation of the optimization problem underlying the PyPSA-Eur framework as used in this study. The presentation closely follows the formulation developed in our previous work [24] and is consistent with the general model descriptions in the PyPSA-Eur literature (e.g., [30,54,55]).

PyPSA-Eur is formulated as a linear cost-minimization problem that determines investment and operation of an interconnected, multi-energy system. The model selects capacities and dispatch for generation, storage, transmission, and conversion technologies such that total annualized system costs (TAC) are minimized. Following [24], the main decision variables include the installed generation capacity $G_{i,\gamma}$, storage energy capacity $S_{i,\sigma}$, transmission line capacity L_j, and the capacity of conversion or transport links (e.g., electrolyzers, heat pumps, HVDC lines, hydrogen pipelines) T_k. Additionally, the dispatch of generators $g_{i,\gamma,\tau}$ and links $t_{k,\tau}$ is optimized for each time step τ.

Total annual system costs comprise annualized capital expenditures (CAPEX) and marginal operating components (OPEX). The objective function is defined in Eq. (A.1), where time-dependent operating costs are weighted by w_τ such that $\sum_{\tau\in\mathcal{T}} w_\tau = 8760\,\mathrm{h}$ [24]:

$$\begin{aligned}\min_{\boldsymbol{G},\boldsymbol{S},\boldsymbol{L},\boldsymbol{T},\boldsymbol{g},\boldsymbol{t}} TAC = &\sum_{i\in\mathcal{I}}\left(\sum_{\gamma\in\Gamma} c_{i,\gamma} G_{i,\gamma} + \sum_{\sigma\in\Sigma} c_{i,\sigma} S_{i,\sigma}\right)\\ &+ \sum_{j\in\mathcal{J}} c_j L_j + \sum_{k\in\mathcal{K}} c_k T_k\\ &+ \sum_{\tau\in\mathcal{T}} w_\tau \left(\sum_{i\in\mathcal{I}}\sum_{\gamma\in\Gamma} o_{i,\gamma} g_{i,\gamma,\tau} + \sum_{k\in\mathcal{K}} o_k t_{k,\tau}\right),\end{aligned} \tag{A.1}$$

where c and o denote annualized investment and marginal operating costs, respectively.

Capacity bounds and dispatch limits

Installed capacities are constrained by exogenously specified limits. Eq. (A.2) enforces these bounds for generation technologies [24]:

$$\underline{G}_{i,\gamma} \le G_{i,\gamma} \le \overline{G}_{i,\gamma} \quad \forall i\in\mathcal{I},\ \gamma\in\Gamma, \tag{A.2}$$

where $\underline{G}_{i,\gamma}$ typically represents existing capacity, and $\overline{G}_{i,\gamma}$ reflects technical expansion potentials (e.g., land availability).

Operational dispatch is restricted by time-dependent availability. As expressed in Eq. (A.3), the feasible dispatch region depends on utilization profiles $\underline{g}_{i,\gamma,\tau}$ and $\overline{g}_{i,\gamma,\tau}$ [24]:

$$\underline{g}_{i,\gamma,\tau} G_{i,\gamma} \le g_{i,\gamma,\tau} \le \overline{g}_{i,\gamma,\tau} G_{i,\gamma} \quad \forall i\in\mathcal{I},\ \gamma\in\Gamma,\ \tau\in\mathcal{T}, \tag{A.3}$$

where $\overline{g}_{i,\gamma,\tau}$ captures, for example, variable renewable availability.

Storage representation

Energy storage operation is bounded by the installed energy capacity $S_{i,\sigma}$. This constraint is given by Eq. (A.4):

$$0 \le s_{i,\sigma,\tau} \le S_{i,\sigma} \quad \forall i\in\mathcal{I},\ \sigma\in\Sigma,\ \tau\in\mathcal{T}. \tag{A.4}$$

Storage dynamics account for self-discharge and net charging flows. The temporal evolution of the state-of-charge follows Eq. (A.5) [24]:

$$s_{i,\sigma,\tau} = s_{i,\sigma,\tau-1}\,\eta_{i,\sigma}^{w_\tau} + w_\tau\,\epsilon_{i,\sigma,\tau} \quad \forall i\in\mathcal{I},\ \sigma\in\Sigma,\ \tau\in\mathcal{T}, \tag{A.5}$$

where $\eta_{i,\sigma}$ is the self-discharge rate and $\epsilon_{i,\sigma,\tau}$ represents the charging/discharging power.

Nodal energy balances

Energy balances ensure supply meets demand at every node and time step. Eq. (A.6) defines this balance, aggregating local generation, storage, and grid inflows [24]:

$$\begin{aligned}\sum_{\gamma\in\Gamma} g_{i,\gamma,\tau} + \sum_{\sigma\in\Sigma} \epsilon_{i,\sigma,\tau} + \sum_{j\in\mathcal{J}} \boldsymbol{K}_{ij}\, l_{j,\tau} + \sum_{k\in\mathcal{K}} \boldsymbol{K}_{ik\tau}\, t_{k,\tau} = d_{i,\tau}\\ \forall i\in\mathcal{I},\ \tau\in\mathcal{T},\end{aligned} \tag{A.6}$$

where $d_{i,\tau}$ is the inelastic demand, and $\boldsymbol{K}_{ij}/\boldsymbol{K}_{ik\tau}$ are incidence matrices mapping line ($l_{j,\tau}$) and link ($t_{k,\tau}$) flows to nodes.

CO_2 emission constraint

Finally, climate targets are enforced via a system-wide emission cap. Eq. (A.7) restricts total annual emissions to the budget $\Lambda_{\mathrm{CO_2}}$ [24]:

$$\sum_{i\in\mathcal{I}}\sum_{\gamma\in\Gamma}\sum_{\tau\in\mathcal{T}} \rho_\gamma\, w_\tau\, g_{i,\gamma,\tau} \le \Lambda_{\mathrm{CO_2}}. \tag{A.7}$$

This compact formulation is directly based on the detailed model description in our earlier study [24] and the established PyPSA-Eur documentation, and is reproduced here to ensure clarity and reproducibility of the present work.

A.2. Heat modeling framework

This section provides an extended overview of the assumptions underlying the (waste) heat modeling framework.

The coefficient of performance (COP) of air- and ground-source heat pumps depends on the respective ambient or soil temperatures and is computed using Eq. (A.8) [56]. Source temperatures T_{source} are derived from ERA5 weather data, while the sink temperature T_{sink} is set to 55 °C.

For the waste-heat heat pump, a COP of 3.175 is assumed, corresponding to a source temperature of 80 °C and a temperature lift to 150 °C [57]. District heating networks are modeled with heat losses of 15%.

$$\begin{aligned}\Delta T &= T_{sink} - T_{source}\\ COP_{ASHP} &= 6.81 - 0.121\Delta T + 0.000630\Delta T^2\\ COP_{GSHP} &= 8.77 - 0.150\Delta T + 0.000734\Delta T^2\end{aligned} \tag{A.8}$$

A.3. Oxygen modeling framework

This section provides an extended overview of the oxygen modeling framework assumptions based on our previous work [24].

Future specific oxygen requirements are modeled assuming parity with current industrial input rates. Table A.1 lists these specific demand figures alongside the requisite argon volumes. Table A.2 further lists specific energy demands and process emissions for each oxygen-related industry sector in 2045.

For methane oxy-fuel combustion, the specific oxygen intensity $D_{\mathrm{O_2}}^{\mathrm{oxy,CH_4}}$ is derived from the fuel's lower heating value ($LHV_{\mathrm{CH_4}}$) and stoichiometric properties. As illustrated in Eq. (A.9) [24], this function incorporates the molar masses M_i and stoichiometric coefficients n_i for both oxygen and methane ($\forall i \in \{\mathrm{O_2}, \mathrm{CH_4}\}$).

$$D_{\mathrm{O_2}}^{\mathrm{oxy,CH_4}} = \frac{M_{\mathrm{O_2}}}{LHV_{\mathrm{CH_4}}\, M_{\mathrm{CH_4}}} \frac{n_{\mathrm{O_2}}}{n_{\mathrm{CH_4}}} \tag{A.9}$$

Table A.1
Overview of the specific base oxygen demands and total argon demand [24].

Industry	Unit	Value	Ref.
Integrated steelworks	t_{O_2}/t_{prod}	0.135 742	Hirth [37], Hegemann and Guder [38]
Electric arc furnaces	t_{O_2}/t_{prod}	0.0536	Toulouevski and Zinurov [58]
Direct reduced iron	t_{O_2}/t_{prod}	0.052 93	Kleimt et al. [59]
Ethylene oxide	t_{O_2}/t_{prod}	0.363[a]	own calc., [40]
Hydrogen peroxide	t_{O_2}/t_{prod}	0.941[a]	own calc., [40]
Sulfuric acid	t_{O_2}/t_{prod}	0.327[a]	own calc., [40]
Pulp production	t_{O_2}/t_{prod}	0.02	Kuparinen et al. [39]
Medical use	t_{O_2}/(a pers)	0.001 112 2	Kato et al. [42]
Other industrial sectors	t_{O_2}/t_{prod}	0.024[b]	own calc.
Argon	Mt_{Ar}/a	0.3	Elsner [31]

[a] Based on stoichiometric reaction ratios.
[b] The value was determined to ensure that, along with other specific demands defined in the model, it results in a total oxygen demand of 9 Mt/a, which corresponds to the German oxygen production in 2017 [41], based on today's industrial production specified in the model.

Table A.2
Specific energy demand and process emissions for each oxygen-related industry sector in 2045 (MWh/t_{prod}; Process emissions in t_{CO_2}/t_{prod}) [30].

Sector	Elec.	Heat	H_2	CH_4	Biomass	Proc. emis.
Steel (Electric Arc)	1.08	–	–	0.19	–	0.04
Steel (DRI)	1.44	–	1.70	0.17	–	0.04
Steel (Integrated)	0.99	0.01	–	0.50	–	0.77
High-value chemicals (HVC)	2.38	0.29	0.16	3.46	0.01	−0.06
Cement	0.10	–	–	0.53	0.20	0.52
Pulp	1.13	0.06	–	0.07	2.27	–
Paper	0.55	0.06	–	0.09	1.99	–
Food & beverages	0.59	0.03	–	0.07	0.59	–
Alumina	1.34	0.03	–	3.53	–	–
Textiles & leather	0.30	0.05	–	0.03	0.24	–
Wood products	0.83	0.06	–	0.02	1.83	–
Other industries	0.24	0.01	–	0.01	0.07	–

Table A.3
Parameter for determining the per capita oxygen and electricity demands for wastewater treatment and oxy-fuel combustion [24].

Parameter	Value	Unit
$BOxD$	300	mg/L
q_{avg}	250	L/(d pers)
$SOTE$	20	%
p_{wwt,O_2}	80	kWh/t_{O_2}
$p_{wwt,air}$	407	kWh/t_{O_2}
$P^{wwt,an}_{el,air}$	55.67	kWh/(a pers)
$P^{wwt,an}_{el,O_2}$	10.96	kWh/(a pers)
$D^{oxy,CH_4}_{O_2}$	0.288	t_{O_2}/MWh_{CH_4}
$D^{oxy,BM}_{O_2}$	0.272	t_{O_2}/MWh_{BM}

The oxygen requirement for biomass combustion, $D^{oxy,bm}_{O_2}$, follows a comparable stoichiometric derivation outlined in Eq. (A.10) [24].

$$D^{oxy,bm}_{O_2} = \frac{n_{O_2,min} M_{O_2}}{HHV_{BM}} D_{BM} \quad (A.10)$$

Regarding wastewater treatment, the annual oxygen load $D^{wwt,an}_{O_2}$ is quantified based on the biochemical oxygen demand $BOxD$, the standard oxygen transfer efficiency $SOTE$, and the average per capita wastewater volume q_{avg}, as expressed in Eq. (A.11) [24].

$$D^{wwt,an}_{O_2} = \frac{BOxD\ q_{avg}}{SOTE} 365\,d/a \quad (A.11)$$

Subsequently, the electrical energy required for aeration $P^{wwt,an}_{el,i}$ is computed by multiplying this total oxygen demand by the specific power consumption of the respective blower technologies $p_{wwt,i}$ ($\forall i \in \{air, O_2\}$), shown in Eq. (A.12) [24].

$$P^{wwt,an}_{el,i} = D^{wwt,an}_{O_2} p_{wwt,i} \quad (A.12)$$

Table A.3 details the numeric parameters utilized in these calculations.

Table A.4 presents the techno-economic parameters of the oxygen-related conversion and storage components. Table A.5 provides the corresponding parameters for oxy-fuel combustion and wastewater treatment processes integrated into the existing model.

Appendix B. Further results

Fig. B.1 shows changes in total annual system costs relative to the base scenario, disaggregated by technology group.

Table B.1 presents the key results of the sensitivity analysis based on variations in the assumed carbon capture and storage (CCS) budget.

Table B.2 details the characteristics of the ten largest electrolyzer locations in the Hybrid scenario, identifying the dominant economic driver based on nodal marginal conditions.

Data availability

The code for the energy system model, along with the results and input data used in this study, is available in a Zenodo repository at https://doi.org/10.5281/zenodo.17241332 under the MIT license.

Code and data for paper: Exploring the impact of synergistic oxygen a nd waste heat utilization from electrolysis in supporting a climate-neu tral energy infrastructure in Germany (Original data) (Zenodo)

Table A.4
Techno-economic parameters of the oxygen-related components. The parameters of the argon storage are based on a generic CO_2 storage tank (ASU: Air Separation Unit) [24].

Component	ASU	Oxygen storage	Argon storage
CAPEX	2.92 M€/(t_{O_2} h)	1670 €/t_{O_2}	2584 €/t_{Ar}
OPEX	4%	1%	1%
Lifetime	25 a	25 a	25 a
Electricity demand	370 kWh_{el}/t_{O_2} [a]		
References	Šulc and Ditl [60], ORLEN [61], Danish Energy Agency [34]	Zeyen et al. [46], Moore et al. [62]	Zeyen et al. [46]

[a] Based on Air Liquide SIGMA plant [60].

Table A.5
Techno-economic parameters of the extended oxygen-related energy system components. The combustion-related costs reflect additional retrofit costs compared to the corresponding process without carbon capture (CC: Carbon Capture, WWT: Wastewater Treatment) [24].

Component		Combustion		WWT	
		Air CC	Oxy-fuel CC	Air	Pure Oxygen
CAPEX	M€/(t_{CO_2} h)	2.0	2.7		
OPEX	$\%_{CAPEX}$	3	3		
Lifetime	a	25	25		
Electricity demand	kWh/(pers a)			55.76	10.96
Oxygen demand	t_{O_2}/(pers a)				0.147
Fuel reductions	%		10/15		
Carbon capture rate	%	90	97		
References		Danish Energy Agency [34], Hofmann et al. [33]	Danish Energy Agency [34], Baukal [35]	Mohammadpour et al. [63]	Mohammadpour et al. [63]

Table B.1
Sensitivity of key results to carbon capture and storage (CCS) limits (100 Mt/a, 70 Mt/a, 50 Mt/a) for the base and hybrid scenario.

CCS limit		100 Mt/a (reference)		70 Mt/a		50 Mt/a	
Parameter	Unit	Base	Hybrid	Base	Hybrid	Base	Hybrid
Electrolysis capacity	GW	99.5	101.4	126.0	125.9	132.1	134.2
H_2 production	TWh/a	302.5	309.6	395.7	398.9	430.9	442.4
WH production	TWh/a	0.0	74.9	0.0	95.8	0.0	106.2
WH integration	TWh/a	0.0	72.8	0.0	95.4	0.0	105.9
O_2 production	Mt/a	0.0	74.3	0.0	95.8	0.0	106.2
O_2 integration	Mt/a	0.0	42.3	0.0	50.3	0.0	53.3
Total system costs	bn €/a	195.0	191.3	204.5	199.6	215.1	209.5
Rel. cost reduction	%	–	**1.9**	–	**2.4**	–	**2.6**
LCOH	€/kg	3.7	3.2	3.9	3.4	3.8	3.3
Rel. LCOH reduction	%	–	**13.0**	–	**11.9**	–	**13.4**

Table B.2
Characteristics and dominant siting drivers for the top 10 electrolyzer nodes in the Hybrid scenario.

Node ID	Region	Capacity [GW]	Elec. price [€/MWh]	H_2 storage [TWh]	Heat dem. [TWh/a]	O_2 dem. [Mt/a]	Dominant driver
50	Mecklenburg (west)	5.5	104	1.7	0.8	0.0	Elec. + storage
82	Lower Saxony (Emsland)	5.4	101	0.6	1.2	0.5	Elec. + storage + O_2 demand
7	Saxony	3.9	106	0.0	7.6	1.0	O_2 + heat synergy
63	Berlin	3.7	105	0.6	10.5	0.1	Storage + heat
53	Lower Saxony (Oldb.)	3.5	102	0.4	2.8	0.3	Elec. + storage + O_2 demand
83	Hamburg	3.3	104	0.5	7.6	0.3	O_2 + heat synergy
96	Brandenburg	2.6	104	0.6	0.6	0.2	Elec. + storage
66	Schleswig-Holstein	2.4	104	1.0	3.0	0.1	Elec. + storage
13	Brandenburg	2.3	105	0.3	8.6	0.2	Heat demand
35	Eastern Ruhr area	2.3	107	0.0	6.0	0.1	Heat demand

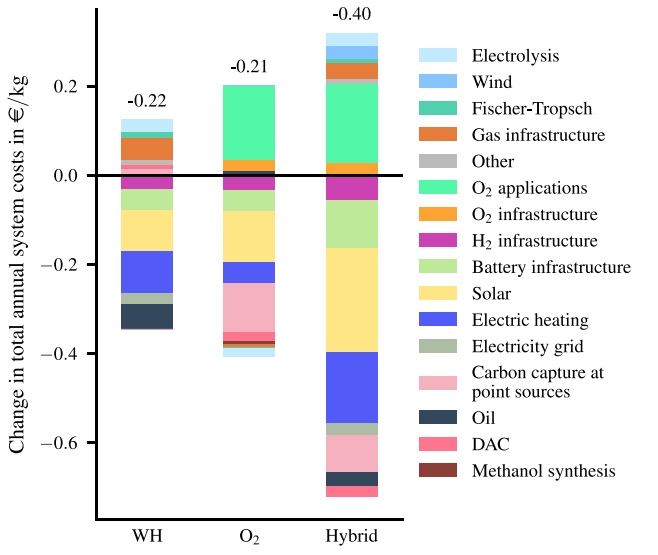

Fig. B.1. Change in total annual system costs relative to the base scenario, disaggregated by technology group. Negative values indicate cost reductions, positive values cost increases. Cost changes are normalized by the corresponding hydrogen production. The net value is shown above the bars. 'Gas infrastructure' and 'Bioenergy' include all methane- and biomass-based combustion technologies without carbon capture. All remaining combustion technologies with carbon capture are grouped under 'Carbon capture at point sources', except for those based on oxy-fuel, which are classified as 'O_2 applications'. 'H_2 infrastructure' mainly includes pipelines and storage (DAC: direct air capture, WH: waste heat, visualization adapted from [33]).

References

[1] Zhu Y, Keoleian GA, Cooper DR. The role of hydrogen in decarbonizing u.s. Industry: A review. Renew Sustain Energy Rev 2025;214:115392. http://dx.doi.org/10.1016/j.rser.2025.115392.

[2] Oliveira AM, Beswick RR, Yan Y. A green hydrogen economy for a renewable energy society. Curr Opin Chem Eng 2021;33:100701. http://dx.doi.org/10.1016/j.coche.2021.100701.

[3] Wappler M, Unguder D, Lu X, Ohlmeyer H, Teschke H, Lueke W. Building the green hydrogen market – current state and outlook on green hydrogen demand and electrolyzer manufacturing. Int J Hydrog Energy 2022;47(79):33551–70. http://dx.doi.org/10.1016/j.ijhydene.2022.07.253.

[4] Buttler A, Spliethoff H. Current status of water electrolysis for energy storage, grid balancing and sector coupling via power-to-gas and power-to-liquids: A review. Renew Sustain Energy Rev 2018;82:2440–54. http://dx.doi.org/10.1016/j.rser.2017.09.003.

[5] Balcombe P, Chatenet M, Deseure J, Schäfer H, Staffell I. Markets and costs for hydrogen electrolysis. In: Bullerdiek N, Neuling U, Kaltschmitt M, editors. Powerfuels: status and prospects. Cham: Springer Nature Switzerland; 2025, p. 235–56. http://dx.doi.org/10.1007/978-3-031-62411-7_9.

[6] Banaszkiewicz T, Chorowski M, Gizicki W. Comparative analysis of cryogenic and PTSA technologies for systems of oxygen production. In: Advances in cryogenic engineering: transactions of the cryogenic engineering conference - CEC. Anchorage, Alaska, USA; 2014, p. 1373–8. http://dx.doi.org/10.1063/1.4860866.

[7] Bo Z, Said MFM, Erdiwansyah E, Mamat R, Xiaoxia J. A review of oxygen generation through renewable hydrogen production. Sustain Chem Clim Action 2025;6:100079. http://dx.doi.org/10.1016/j.scca.2025.100079.

[8] Serrano J, Martín J, Gomez-Soriano J, Raggi R. Theoretical and experimental evaluation of the spark-ignition premixed oxy-fuel combustion concept for future CO2 captive powerplants. Energy Convers Manage 2021;244:114498. http://dx.doi.org/10.1016/j.enconman.2021.114498.

[9] Rusmanis D, Yang Y, Lin R, Wall DM, Murphy JD. Operation of a circular economy, energy, environmental system at a wastewater treatment plant. Adv Appl Energy 2022;8:100109. http://dx.doi.org/10.1016/j.adapen.2022.100109.

[10] Böhm H, Moser S, Puschnigg S, Zauner A. Power-to-hydrogen & district heating: technology-based and infrastructure-oriented analysis of (future) sector coupling potentials. Int J Hydrog Energy 2021;46(63):31938–51. http://dx.doi.org/10.1016/j.ijhydene.2021.06.233.

[11] Rehfeldt M, Fleiter T, Toro F. A bottom-up estimation of the heating and cooling demand in European industry. Energy Effic 2018;11(5):1057–82. http://dx.doi.org/10.1007/s12053-017-9571-y.

[12] Klute S, Budt M, Van Beek M, Doetsch C. Steam generating heat pumps – overview, classification, economics, and basic modeling principles. Energy Convers Manage 2024;299:117882. http://dx.doi.org/10.1016/j.enconman.2023.117882.

[13] Meriläinen A, Kosonen A, Jokisalo J, Kosonen R, Kauranen P, Ahola J. Techno-economic evaluation of waste heat recovery from an off-grid alkaline water electrolyzer plant and its application in a district heating network in Finland. Energy 2024;306:132181. http://dx.doi.org/10.1016/j.energy.2024.132181.

[14] Neumann F, Zeyen E, Victoria M, Brown T. The potential role of a hydrogen network in europe. Joule 2023;7(8):1793–817. http://dx.doi.org/10.1016/j.joule.2023.06.016.

[15] Heitkoetter W, Medjroubi W, Vogt T, Agert C. Regionalised heat demand and power-to-heat capacities in Germany – an open dataset for assessing renewable energy integration. Appl Energy 2020;259:114161. http://dx.doi.org/10.1016/j.apenergy.2019.114161.

[16] Assunção R, Eckl F, Ramos CP, Correia CB, Neto RC. Oxygen liquefaction economical value in the development of the hydrogen economy. Int J Hydrog Energy 2024;62:109–18. http://dx.doi.org/10.1016/j.ijhydene.2024.02.205.

[17] Maggio G, Squadrito G, Nicita A. Hydrogen and medical oxygen by renewable energy based electrolysis: A green and economically viable route. Appl Energy 2022;306:117993. http://dx.doi.org/10.1016/j.apenergy.2021.117993.

[18] Frassl N, Sistani NR, Wimmer Y, Kapeller J, Maggauer K, Kathan J. Techno-economic assessment of waste heat recovery for green hydrogen production: A simulation study. E+I Elektrotechnik Informationstechnik 2024;141(5):288–98. http://dx.doi.org/10.1007/s00502-024-01231-y.

[19] van der Roest E, Bol R, Fens T, van Wijk A. Utilisation of waste heat from PEM electrolysers – unlocking local optimisation. Int J Hydrog Energy 2023;48(72):27872–91. http://dx.doi.org/10.1016/j.ijhydene.2023.03.374.

[20] Hönig F, Rupakula GD, Duque-Gonzalez D, Ebert M, Blum U. Enhancing the levelized cost of hydrogen with the usage of the byproduct oxygen in a wastewater treatment plant. Energies 2023;16(12):4829. http://dx.doi.org/10.3390/en16124829.

[21] Ferraro M, Massaro F, Sanseverino ER, Ruffino S. Is selling the oxygen produced during electrolysis really a solution to make green hydrogen cheaper? In: 2024 IEEE international conference on environment and electrical engineering and 2024 IEEE industrial and commercial power systems europe (EEEIC / i&CPS europe). 2024, p. 1–6. http://dx.doi.org/10.1109/EEEIC/ICPSEurope61470.2024.10751545.

[22] Donald R, Love JG. Energy shifting in wastewater treatment using compressed oxygen from integrated hydrogen production. J Environ Manag 2023;331:117205. http://dx.doi.org/10.1016/j.jenvman.2022.117205.

[23] Nhuchhen DR, Sit SP, Layzell DB. Decarbonization of cement production in a hydrogen economy. Appl Energy 2022;317:119180. http://dx.doi.org/10.1016/j.apenergy.2022.119180.

[24] Bornemann L, Lange J, Kaltschmitt M. Oxygen production via electrolysis: A model-based assessment of its impact on a climate-neutral german energy system. Energy Convers Manage 2025;344:120213. http://dx.doi.org/10.1016/j.enconman.2025.120213.

[25] Campbell-Stanway C, Becerra V, Prabhu S, Bull J. Investigating the role of byproduct oxygen in UK-based future scenario models for green hydrogen electrolysis. Energies 2024;17(2):281. http://dx.doi.org/10.3390/en17020281.

[26] Galvan-Cara A-L, Bongartz D. Rethinking electrolyzer design for optimal waste-heat utilization. Appl Energy 2025;398:126367. http://dx.doi.org/10.1016/j.apenergy.2025.126367.

[27] Gómez de Arteche-Botas M, Iturralde- Iñarga J, Fúnez-Guerra C. Heat pump integration for waste heat recovery from a 20 MWe green hydrogen plant to increase global efficiency. Int J Hydrog Energy 2025;142:777–83. http://dx.doi.org/10.1016/j.ijhydene.2025.04.202.

[28] Lungu F-A, Patularu L, Nasture A, Carcadea E, Hoarcă IC, Şerbănescu M. Waste heat recovery for a PEM electrolyzer. In: 2025 17th international conference on electronics, computers and artificial intelligence (ECAI). 2025, p. 1–5. http://dx.doi.org/10.1109/ECAI65401.2025.11095451.

[29] Pompodakis EE, Ahmed A, Orfanoudakis GI, Karapidakis ES. Optimization of residential hydrogen facilities with waste heat recovery: economic feasibility across various European cities. Processes 2024;12(9):1933. http://dx.doi.org/10.3390/pr12091933.

[30] Neumann F, Zeyen E, Victoria M, Brown T. The potential role of a hydrogen network in europe. Joule 2023;7(8):1793–817. http://dx.doi.org/10.1016/j.joule.2023.06.016.

[31] Elsner H. Edelgase – versorgung wirklich kritisch? – DERA rohstoffinformationen 39. Technical Report, Berlin: Deutsche Rohstoffagentur (DERA); 2018, p. 196.

[32] Government GF. Climate change act 2021. 2021.

[33] Hofmann F, Tries C, Neumann F, Zeyen E, Brown T. H_2 and CO_2 network strategies for the European energy system. Nat Energy 2025;10(6):715–24. http://dx.doi.org/10.1038/s41560-025-01752-6.

[34] Danish Energy Agency. Technology data – carbon capture, transport and storage. 2024.

[35] Baukal Jr CE. Oxygen-enhanced combustion, second ed.. Industrial combustion series, Boca Raton: CRC Press. Taylor & Francis Group; 2013, http://dx.doi.org/10.1201/b13974.
[36] Wei X, Manovic V, Hanak DP. Techno-economic assessment of coal- or biomass-fired oxy-combustion power plants with supercritical carbon dioxide cycle. Energy Convers Manage 2020;221:113143. http://dx.doi.org/10.1016/j.enconman.2020.113143.
[37] Hirth T. Super – sustainable production, energy and resources. Chem Ing Tech 2012;84(7). http://dx.doi.org/10.1002/cite.201290061, 943–943.
[38] Hegemann K-R, Guder R. Stahlerzeugung. Wiesbaden: Springer Fachmedien Wiesbaden; 2020, http://dx.doi.org/10.1007/978-3-658-29091-7.
[39] Kuparinen K, Vakkilainen E, Ryder P. Integration of electrolysis to produce hydrogen and oxygen in a pulp mill process. Appita: Technol Innov Manuf Environ 2016;69(1):81–8.
[40] Verband der Chemischen Industrie eV(VCI). Produktion anorganischer grundchemikalien in deutschland 2022 und 2023. Statista 2024.
[41] Verband der Chemischen Industrie eV(VCI). Chemiewirtschaft in zahlen - 2024. 2024.
[42] Kato T, Kubota M, Kobayashi N, Suzuoki Y. Effective utilization of by-product oxygen from electrolysis hydrogen production. In: International energy workshop, Energy In: International energy workshop, 2005;30(14):2580–95.http://dx.doi.org/10.1016/j.energy.2004.07.004,
[43] Schlachtberger D, Brown T, Schäfer M, Schramm S, Greiner M. Cost optimal scenarios of a future highly renewable European electricity system: exploring the influence of weather data, cost parameters and policy constraints. Energy 2018;163:100–14. http://dx.doi.org/10.1016/j.energy.2018.08.070.
[44] Pfeifroth U, Kothe S, Müller R, Trentmann J, Hollmann R, Fuchs P, Werscheck M. Surface radiation data set - heliosat (SARAH) - edition 2. 2017, http://dx.doi.org/10.5676/EUM_SAF_CM/SARAH/V002.
[45] Hersbach H, Bell B, Berrisford P, Hirahara S, Horányi A, Muñoz-Sabater J, Nicolas J, Peubey C, Radu R, Schepers D, Simmons A, Soci C, Abdalla S, Abellan X, Balsamo G, Bechtold P, Biavati G, Bidlot J, Bonavita M, De Chiara G, Dahlgren P, Dee D, Diamantakis M, Dragani R, Flemming J, Forbes R, Fuentes M, Geer A, Haimberger L, Healy S, Hogan RJ, Hólm E, Janisková M, Keeley S, Laloyaux P, Lopez P, Lupu C, Radnoti G, De Rosnay P, Rozum I, Vamborg F, Villaume S, Thépaut J-N. The ERA5 global reanalysis. Q J R Meteorol Soc 2020;146(730):1999–2049. http://dx.doi.org/10.1002/qj.3803.
[46] Zeyen E, Neumann F, Millinger M, Parzen M, aalamia, Franken L, Brown T, Geis J, Glaum P, martavp, cpschau, van Greevenbroek K, Trippe L, fhg-isi, lukasnacken, s8au, Seibold T. PyPSA/technology-data: V0.9.1. Zenodo; 2024, http://dx.doi.org/10.5281/ZENODO.13255345.
[47] Danish Energy Agency. Technology catalogues. 2024.
[48] Mantzos L, Matei NA, Mulholland E, Rózsai M, Tamba M, Wiesenthal T. JRC-IDEES 2015. European Commission, Joint Research Centre (JRC); 2018, http://dx.doi.org/10.2905/JRC-10110-10001.
[49] Pia Manz TF. Georeferenced industrial sites with fuel demand and excess heat potential. Zenodo; 2018, http://dx.doi.org/10.5281/ZENODO.4687147.
[50] Muehlenpfordt J. Time series. Open Power System Data; 2019, http://dx.doi.org/10.25832/TIME_SERIES/2019-06-05.
[51] Eurostat. Complete energy balances. Eurostat; 2022, http://dx.doi.org/10.2908/NRG_BAL_C.
[52] Federal Ministry for Economic Affairs and Climate Action (BMWK). Fortschreibung der nationalen wasserstoffstrategie. 2023.
[53] European Commission. Repowereu plan. COM/2022/230 final. 2022.
[54] Hörsch J, Hofmann F, Schlachtberger D, Brown T. Pypsa-eur: an open optimisation model of the European transmission system. Energy Strat Rev 2018;22:207–15. http://dx.doi.org/10.1016/j.esr.2018.08.012.
[55] Brown T, Victoria M, Zeyen E, Hofmann F, Neumann F, Frysztacki M, Hampp J, Schlachtberger D, Hörsch J. Pypsa-eur: an open sector-coupled optimisation model of the European energy system. 2024, http://dx.doi.org/10.5281/ZENODO.11305883.
[56] Hörsch J, Hofmann F, Schlachtberger D, Brown T. Pypsa-eur documentation. 2024.
[57] Danish Energy Agency. Technology data – industrial process heat. 2024.
[58] Toulouevski YN, Zinurov IY. Modern steelmaking in electric arc furnaces: history and development. In: Toulouevski YN, Zinurov IY, editors. Innovation in electric arc furnaces: scientific basis for selection. Berlin, Heidelberg: Springer; 2013, p. 1–24. http://dx.doi.org/10.1007/978-3-642-36273-6_1.
[59] Kleimt B, Dettmer B, Haverkamp V, Deinet T, Tassot P. Erhöhung der energie-und materialeffizienz der stahlerzeugung im lichtbogenofen. 2012, http://dx.doi.org/10.1002/cite.201200076.
[60] Šulc R, Ditl P. A technical and economic evaluation of two different oxygen sources for a small oxy-combustion unit. J Clean Prod 2021;309:127427. http://dx.doi.org/10.1016/j.jclepro.2021.127427.
[61] ORLEN. Agreement for building of the new air separation unit III in the production plant in plock. 2022.
[62] Moore JJ, Pryor O, Cormier I, Fetvedt J. Oxygen storage incorporated into net power and the allam–fetvedt oxy-fuel sCO2 power cycle—techno-economic analysis. J Eng Gas Turbines Power 2024;146(091021). http://dx.doi.org/10.1115/1.4065048.
[63] Mohammadpour H, Cord-Ruwisch R, Pivrikas A, Ho G. Utilisation of oxygen from water electrolysis – assessment for wastewater treatment and aquaculture. Chem Eng Sci 2021;246:117008. http://dx.doi.org/10.1016/j.ces.2021.117008.